

Mean Field Approximation of IIB Matrix Model and Emergence of Four Dimensional Space-Time

H. KAWAI^{a*}, S. KAWAMOTO^{a†}, T. KUROKI^{a‡},
T. MATSUO^{b§} and S. SHINOHARA^{a¶}

^a*Department of Physics, Kyoto University, Kyoto 606-8502, Japan*

^b*Yukawa Institute for Theoretical Physics, Kyoto University,
Kyoto 606-8502, Japan*

April, 2002

Abstract

For the purpose of analyzing non-perturbative dynamics of string theory, Nishimura and Sugino have applied an improved mean field approximation (IMFA) to IIB matrix model. We have extracted the essence of the IMFA and obtained a general scheme, the improved Taylor expansion, that can be applied to a wide class of series which is not necessarily convergent. This approximation scheme with the help of the 2PI free energy enables us to perform higher order calculations. We have shown that the value of the free energy is stable at higher orders, which supports the validity of the approximation. Moreover, the ratio between the extent of “our” space-time and that of the internal space is found to increase rapidly as we take the higher orders into account. Our results suggest that the four dimensional space-time emerges spontaneously in IIB matrix model.

*hkawai@gauge.scphys.kyoto-u.ac.jp

†kawamoto@gauge.scphys.kyoto-u.ac.jp

‡kuroki@gauge.scphys.kyoto-u.ac.jp

§tmatsuo@yukawa.kyoto-u.ac.jp

¶shunichi@gauge.scphys.kyoto-u.ac.jp

1 Introduction and summary

After the enormous success in revealing perturbative dynamics of string theory with/without D-branes [1, 2, 3, 4], our focus will go on to the full non-perturbative dynamics, or to the theory which has predictive power for the real world.

In such a stage, both a model which is to be the true theory and a method to extract non-perturbative information from it are important. Some models have already been conjectured as the constructive definition of string theory and/or quantum gravity [5, 6, 7, 8, 9]. Among others we are interested in IIB matrix model [6, 10] which would be the most promising to attack the non-perturbative dynamics of string theory.

As to the method, J. Nishimura and F. Sugino [11] have applied an improved mean field approximation (IMFA) [12] to IIB matrix model with an excellent idea for breaking the Lorentz symmetry, and suggested that the four dimensional space-time is more stable than those of the other dimensions. In sec. 2, we review the IMFA with an application to a toy model. Although the IMFA is somewhat mysterious, we find that the essential feature of the IMFA can be captured in terms of the improved Taylor expansion (ITE) which is elucidated in sec.3. In [11] the authors have calculated to the third order and got a result which is both remarkable and uneasy:

remarkable fact Even at the third order, non-perturbative aspects of IIB matrix model can be captured definitely.

uneasy fact Not knowing the stability of the result, we can not strongly believe it.

To confirm the validity of the IMFA for IIB matrix model, we should investigate the stability of the result, especially the free energy, as we increase the order of approximation. The aim of this paper is to deepen the remarkable aspect and to remove the uneasy problem at a time. So we proceed to the next order calculation. Since Feynman graphs to be calculated increase in number and become complicated, we need to introduce a new method. It turns out nice to use the two-particle irreducible (2PI) free energy which is explained in sec. 4. With the help of the 2PI free energy we have completed the fifth order calculation and see how the above aim is achieved. We find that the contribution of the fifth order to the free energy is smaller than that of the third order, which supports the validity of this approximation.

The ratio between the extent of the four dimensional space-time and that of the extra internal space is found to increase from three (the third order) to six (the fifth order) as is

shown in sec. 5. This indicates that the ratio is infinite in the full theory and the flat four dimensional space-time is generated.

2 Improved mean field approximation

2.1 general prescription

Suppose we have some action function $S(x)$ and its partition function

$$Z = \int dx e^{-S(x)}. \quad (2.1)$$

In general, this integral can not be performed analytically, and we need an approximation scheme to evaluate the partition function. In the mean field approximation, we add the mean field action $S_0(x; a)$ which can be integrated analytically, and subtract it as an interaction term. The mean field action contains a set of parameters a which should be determined later according to the order of the approximation. The original action $S(x)$ is also treated as an interaction term. Here we introduce a coupling g formally, which will be set to 1 at the end of the calculation. To get the k -th order approximation, we convert the expression to a formal power series with respect to g and truncate it up to order k . The prescription is as follows:

$$Z = \int dx e^{-S_0(x; a) - g(S(x) - S_0(x; a))} \quad (2.2)$$

↓ convert to the formal power series w.r.t. g

$$Z \sim \sum_{n=0}^{\infty} \frac{(-g)^n}{n!} \int dx (S(x) - S_0(x; a))^n e^{-S_0(x; a)} \quad (2.3)$$

↓ truncate the summation

$$Z_k(a) = \sum_{n=0}^k \frac{(-g)^n}{n!} \int dx (S(x) - S_0(x; a))^n e^{-S_0(x; a)}. \quad (2.4)$$

The truncated partition function $Z_k(a)$ is a function of the parameters a , though the original partition function is independent of them. Thus we can determine the values of the parameters so that the truncated partition function is stationary with respect to a . We call this procedure the improved mean field approximation (IMFA).

To approximate the correlation function, we use the same truncation:

$$\langle f(x) \rangle_k = \frac{1}{Z_k(a)} \sum_{n=0}^k \frac{(-g)^n}{n!} \int dx f(x) (S(x) - S_0(x; a))^n e^{-S_0(x; a)} \Bigg|_{\text{neglect } O(g^{k+1})}. \quad (2.5)$$

Note that at the first order IMFA is the same as the variational principle. Note also that the power series (2.3) is in general only an asymptotic series if we fix the parameter a . Nevertheless by determining a order by order, we can approximate the original partition function with high accuracy as we will see in the next subsection.

2.2 application to a toy model

As an example, let us apply the IMFA to the zero dimensional ϕ^4 model whose partition function can be integrated exactly. The action is

$$S = \frac{m^2}{2}\phi^2 + \frac{\lambda}{4!}\phi^4. \quad (2.6)$$

The exact values of the partition function and the two point function in the massless case ($m^2 = 0, \lambda = 1$) in which we are especially interested are

$$Z_{\text{massless}} = \int d\phi e^{-S} = 2 \cdot 3! \cdot (4!)^{-3/4} \cdot \Gamma(1/4), \quad (2.7)$$

$$F_{\text{massless}} = -\log Z \simeq -1.389388802, \quad (2.8)$$

$$\langle \phi^2 \rangle_{\text{massless}} = \frac{1}{Z} \int d\phi \phi^2 e^{-S} = (4!)^{1/2} \frac{\Gamma(3/4)}{\Gamma(1/4)} \simeq 1.655801764. \quad (2.9)$$

We adopt the following action as S_0 ,

$$S_0 = \frac{m_0^2}{2}\phi^2, \quad (2.10)$$

where m_0^2 is a variational parameter which corresponds to a in the previous subsection. Even in the massless case, this action enables us to calculate the free energy $F_k = -\log Z_k$ by using the ordinary Feynman diagrams.

Graphically, F_k is the sum of all connected vacuum graphs shown as in eq. (2.11), where a line and a cross with a circle represent a propagator $1/m_0^2$ and a mass counter term $g(m_0^2 - m^2)$ respectively. The four-point vertex denotes $g\lambda$.

$$F = \underbrace{\bigcirc}_{O(g^0)} + \underbrace{\left(\begin{array}{c} \bigcirc \\ \bigcirc \end{array} + \begin{array}{c} \bigcirc \\ \times \end{array} \right)}_{O(g^1)} + \underbrace{\left(\begin{array}{c} \bigcirc \\ \bigcirc \\ \bigcirc \end{array} + \begin{array}{c} \bigcirc \\ \bigcirc \\ \bigcirc \\ \bigcirc \end{array} + \begin{array}{c} \bigcirc \\ \times \\ \bigcirc \end{array} + \begin{array}{c} \bigcirc \\ \times \\ \times \\ \bigcirc \end{array} \right)}_{O(g^2)} + \dots \quad (2.11)$$

Figs.1 and 2 show the approximated free energies and two point functions as functions of m_0^2 in the massless case. We find that the higher the order of the approximation, the wider the plateau at the exact values in both cases. This phenomenon is expected because the free energy F should not depend on the parameter m_0^2 which is introduced artificially. Although the truncated free energy F_k depends on m_0^2 , we expect m_0^2 dependence becomes weaker for larger values of k . Since the truncated free energies and two point functions are merely polynomials in $1/m_0^2$, the existence of the plateau indicates that extremum points of these polynomials concentrate on limited regions. Once the plateau exists, small changes of m_0^2 do not affect the resultant values. Therefore if we have a plateau, we can regard the value in the region as a good approximation of the exact value.

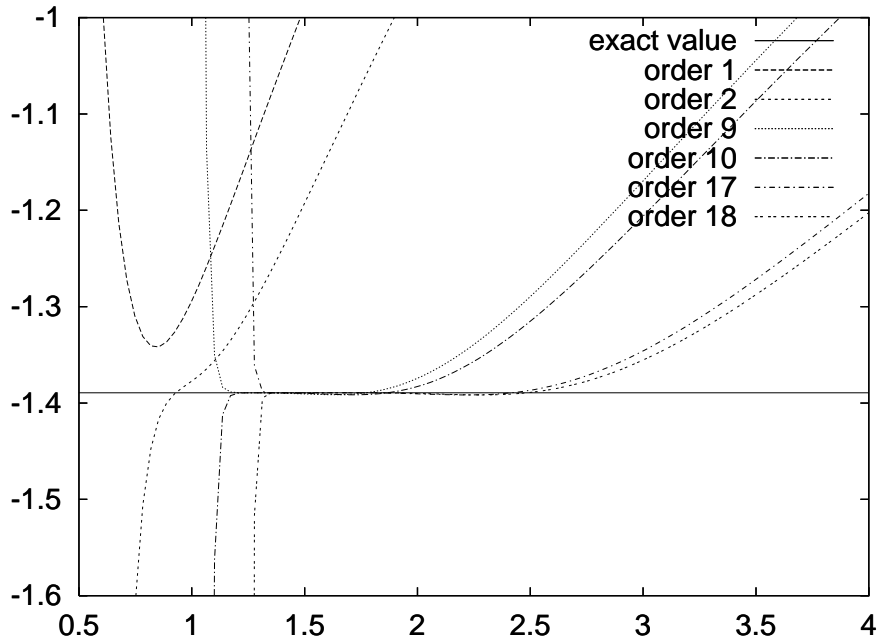


Figure 1: Truncated free energies in the IMFA scheme. The horizontal axis denotes m_0^2 .

3 Improved Taylor expansion

The IMFA is a rather curious approximation scheme. It is interesting to understand the ground on which it works. In this section, we see that the improved Taylor expansion (ITE) explains some of the essential aspects of the IMFA.

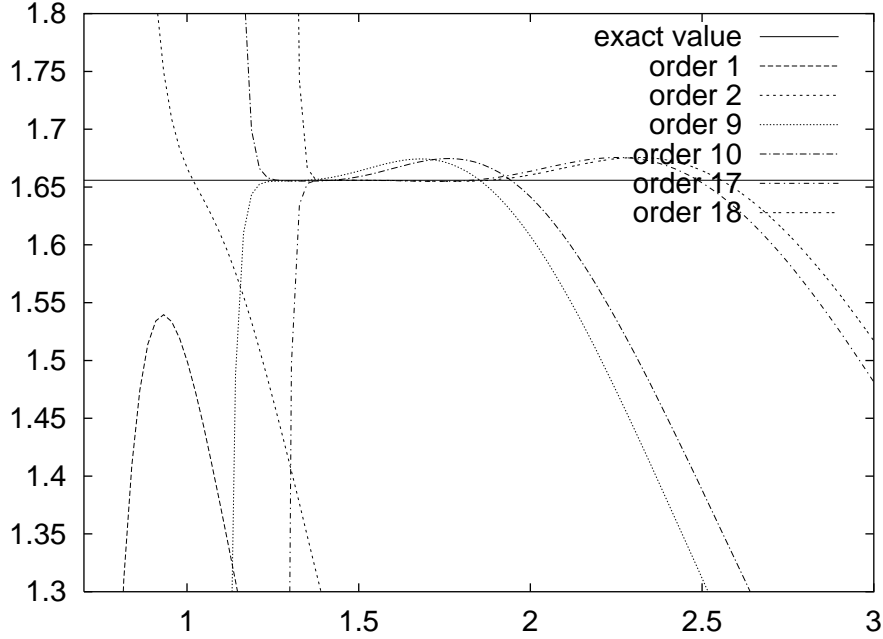


Figure 2: Truncated two point functions in the IMFA scheme. The horizontal axis is m_0^2 .

Suppose we have a sequence of functions $\{f_i(x)\}_{i=0,1,\dots}$ which does not necessarily converge. We define an improved sequence $\{f_i^{\text{improved}}(x; x_0)\}_{i=0,1,\dots}$ by

$$f_i^{\text{improved}}(x; x_0) = \sum_{n=0}^i \frac{1}{n!} (x - x_0)^n f_{i-n}^{(n)}(x_0). \quad (3.1)$$

We call this prescription the improved Taylor expansion (ITE). We emphasize that each f_i^{improved} is constructed from finite number of f_j 's, that is, f_0, f_1, \dots, f_i . This differs from the ordinary Taylor expansion in that we use f_j with smaller j 's for higher derivative terms. As we see below, different values of x_0 make $\{f_i^{\text{improved}}\}_{i=0,1,\dots}$ converge in different regions. This property enables us to obtain a series which converges around various values of x by choosing proper x_0 correspondingly.

For example, we consider a power series given by

$$f(x) = \sum_{n=0}^{\infty} (-)^n x^n (= \frac{1}{1+x}), \quad (3.2)$$

and define $\{f_i\}_{i=0,1,\dots}$ by

$$f_i = \sum_{n=0}^i (-)^n x^n. \quad (3.3)$$

The behavior of this sequence $\{f_i\}_{i=0,1,\dots}$ is shown in Fig.3, which manifests that the convergence radius of the series is 1. The improved sequence $\{f_i^{\text{improved}}(x; x_0)\}_{i=0,1,\dots}$ for $x_0 = 1.1$,

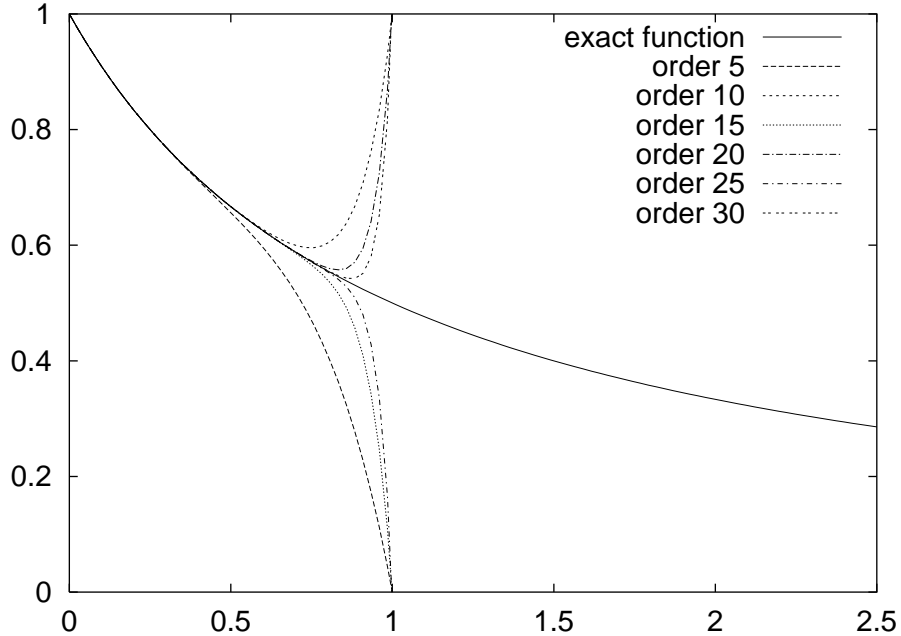


Figure 3: Original series. The horizontal axis is x .

for instance, behaves as in Fig.4. This sequence converges well around $x \sim 3/2$. Thus the improved sequence has a totally different convergence region from that of the original sequence. As we can see from this example, the reason why we use f_j with smaller j 's in the definition of the ITE eq. (3.1) is that f_j with the higher j 's make behavior of the sum worse for a divergent series.

To see the relation with the IMFA more clearly, let us fix x to $3/2$, outside the convergent radius (x corresponds to m^2 in eq. (2.6)). Instead we regard $f_i^{\text{improved}}(3/2; x_0)$ as a function of x_0 . Now x_0 corresponds to a parameter in the IMFA (m_0^2 in eq. (2.10)). As seen from Fig.5, there are plateaus on the exact value $f(3/2) = 0.4$. The plateau gets wider as we increase the order of the approximation. The approximation is nice and the improved functions are almost independent of the variational parameter x_0 as expected.

The expansion (3.1) can be written in a concise form. First, we introduce a formal expansion

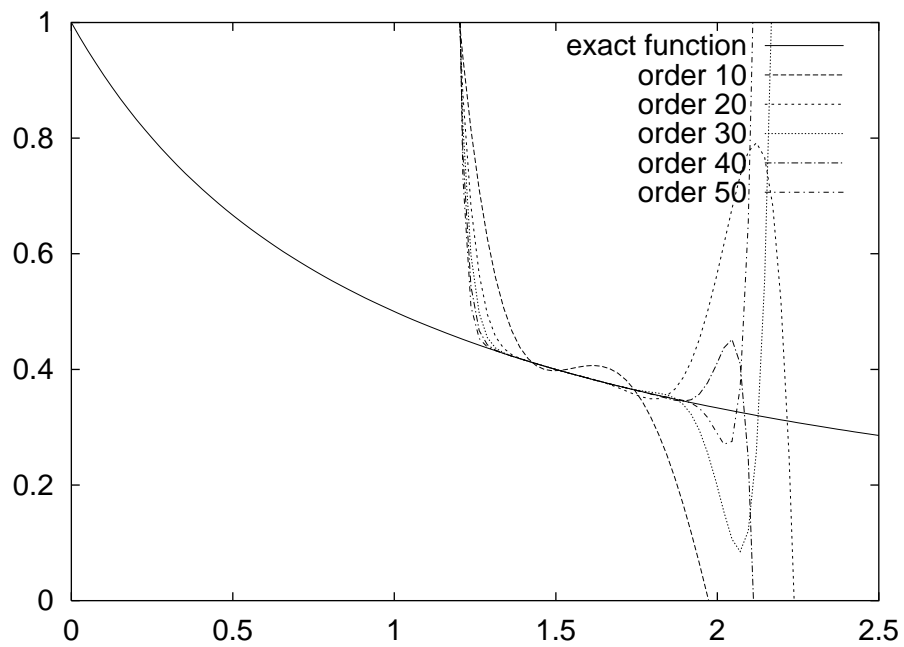


Figure 4: ITE around $x_0 = 1.1$. The horizontal axis is x .

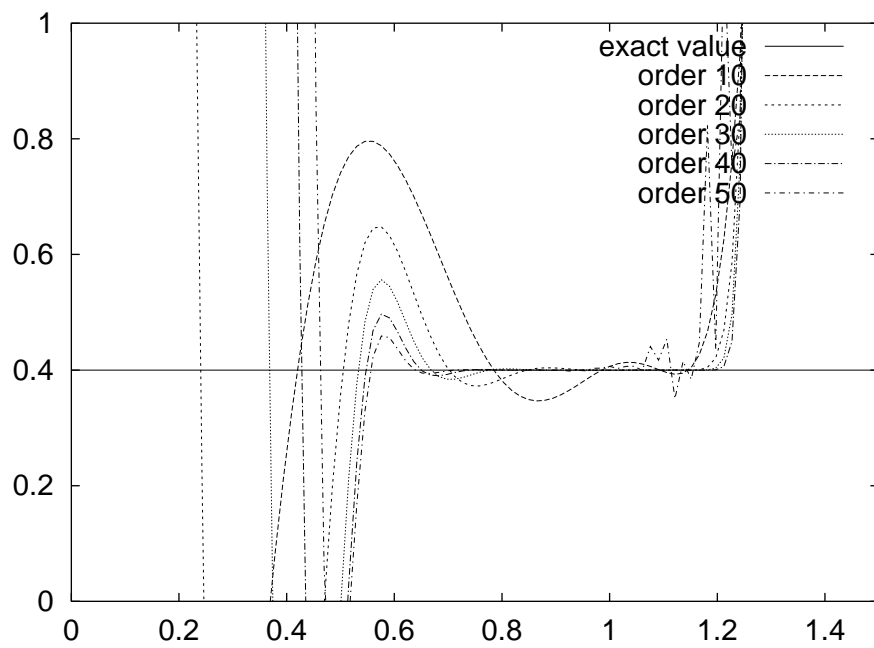


Figure 5: The plateau in ITE scheme. The horizontal axis is x_0 .

sion parameter g , and define a function from the sequence of functions $\{f_i(x)\}_{i=0,1,\dots}$,

$$f(x) = \sum_{i=0}^{\infty} g^i h_i(x), \quad (3.4)$$

where $h_i(x) = f_i(x) - f_{i-1}(x)$ ($i = 1, 2, \dots$) and $h_0(x) = f_0(x)$. For example, in the case of power series eq. (3.2) we have $h_i(x) = (-)^i x^i$. Next we substitute $x_0 + g(x - x_0)$ for x in this $f(x)$ and truncate it with respect to g :

$$f_i^{\text{improved}}(x; x_0) = f(x_0 + g(x - x_0)) \Big|_i. \quad (3.5)$$

Here $|_i$ denotes neglecting $O(g^{i+1})$ terms and setting $g=1$. One can easily verify that this expression reproduces the functions in the improved sequence eq. (3.1).

In relation to the IMFA, the derivatives correspond to insertions of mass counter terms. As a result, the IMFA is included in a more general scheme, the ITE. The abstract feature of the ITE may be useful to find the essence of the IMFA. Once we understand the essence, we could refine the IMFA in various ways and use a refined method to grasp the non-perturbative properties of IIB matrix model further.

For reference, some curious behavior of the ITE and an application to an asymptotic series are examined in appendices A and B.

4 2PI free energy and Legendre transformation

In the application of the IMFA to various models, we can drastically simplify the computation by using the 2PI free energy. In this paper, we apply the Legendre transformation to the 2PI free energy to obtain the ordinary free energy, and search its extrema.

Although within this procedure the 2PI free energy seems just a technical tool, we can give it a more fundamental meaning related to the Schwinger-Dyson equations (SDE). In fact, we can apply the ITE scheme directly to the 2PI free energy, which we explain in appendix C.

4.1 Schwinger-Dyson equations and 2PI free energy

The SDE are the consistency conditions among the Green functions and in some cases we can extract non-perturbative information from them. Again we consider the massless ϕ^4 model.

For the full propagator $c = \langle \phi^2 \rangle$, we can derive the SDE as shown in eq. (4.1).

$$0 = \frac{1}{\bullet \text{---} \boxed{} \text{---} \bullet} + \frac{\text{---} \circ \text{---}}{\text{---} \boxed{} \text{---}} + \frac{\text{---} \circ \text{---}}{\text{---} \boxed{} \text{---}} + \dots \quad (4.1)$$

The derivation of this equation is given in appendix F. Note that each graph has no self-energy part when we regard each full propagator as a single line.

This equation is, in fact, the stationary condition of the two particle irreducible (2PI) free energy which we call G hereafter.

$$G = \text{---} \circ \text{---} + \text{---} \circ \text{---} + \text{---} \circ \text{---} + \dots \quad (4.2)$$

2PI graphs are the ones that remain connected after cutting any two distinct propagators. In other words, 2PI graphs do not contain any self-energy part as a subgraph. This property comes from the fact that the SDE do not contain any self-energy part. The correspondence between the SDE for the full propagators and the 2PI free energy holds generally in field theory.

The advantage of considering the 2PI free energy is that we can greatly reduce the number of graphs. Next, we will explain the relation between the 2PI free energy and the ordinary free energy.

4.2 Legendre transformation

Let us start with the free energy,

$$Z(J) = \int d\phi e^{-S(\phi) - J\phi^2}, \quad (4.3)$$

$$F(J) = -\log Z(J). \quad (4.4)$$

Here we introduce a source J for ϕ^2 . We apply the Legendre transformation to $F(J)$ with respect to J .

$$K(J) = \frac{\partial F(J)}{\partial J}, \quad (4.5)$$

$$G(K) = \left[F(J) - J \frac{\partial F(J)}{\partial J} \right]_{J=J(K)}, \quad (4.6)$$

where K is the conjugate variable of J . To investigate the original theory, we set $J = 0$. Then $K(J = 0)$ is equal to the full two-point function c ,

$$K(J = 0) = \langle \phi^2 \rangle_{J=0} = c, \quad (4.7)$$

and $G(K = c)$ is nothing but the sum of the 2PI vacuum graphs [13].

For example, we use this procedure for the ϕ^4 model, eq. (2.6). The free energy F is given by the sum of the connected vacuum graphs,

$$F = \frac{1}{2} \log(m^2 + 2J) + \frac{\lambda}{8} \frac{1}{(m^2 + 2J)^2} - \lambda^2 \left(\frac{1}{48} + \frac{1}{16} \right) \frac{1}{(m^2 + 2J)^4} + O(\lambda^3), \quad (4.8)$$

where each term corresponds to the one in eq. (2.11) other than the graphs with mass counter terms. The full propagator becomes as follows:

$$c = \frac{1}{m^2} - \frac{\lambda}{2} \frac{1}{(m^2)^3} + \lambda^2 \frac{2}{3} \frac{1}{(m^2)^5} + O(\lambda^3). \quad (4.9)$$

This equation can be solved with respect to $1/m^2$ iteratively, and we get the 2PI free energy G .

$$\frac{1}{m^2} = c + \frac{\lambda}{2} c^3 + \frac{\lambda^2}{12} c^5 + O(\lambda^3), \quad (4.10)$$

$$G = -\frac{1}{2} - \frac{1}{2} \log c + \frac{1}{2} c m^2 + \frac{\lambda}{8} c^2 - \frac{\lambda^2}{48} c^4 + O(\lambda^3), \quad (4.11)$$

which reproduces eq. (4.2) correctly when $m^2 = 0$ ¹.

In the practical calculations, it is easier to compute the 2PI free energy $G(c)$ first and then obtain $F(m^2)$ by applying the inverse Legendre transformation to $G(c)$.

Once we obtain the free energy $F(m^2)$, we replace λ with $g\lambda$ and apply the ITE with respect to m^2 . For example if we consider the massless case corresponding to IIB matrix model, the improved free energies are

$$F_k^{\text{improved}} = F(m_0^2 - gm_0^2)|_k \quad (4.12)$$

$$= -\frac{1}{2} \log c_0 + g \left(\frac{\lambda}{8} c_0^2 - \frac{1}{2} \right) + g^2 \left(-\frac{\lambda^2}{48} c_0^4 - \frac{\lambda^2}{16} c_0^4 + \frac{\lambda}{4} c_0^2 - \frac{1}{4} \right) + \dots \Big|_k, \quad (4.13)$$

where c_0 stands for $1/m_0^2$. Again, the last equation is the same as eq. (2.11) term by term.

¹Here an additive constant is not important.

5 The ansatz and the results

5.1 IIB matrix model

Our aim is to analyze IIB matrix model [6]. The action is

$$S = -\frac{1}{g_0^2} \text{Tr} \left(\frac{1}{4} [A_\mu, A_\nu]^2 - \frac{1}{2} \bar{\psi} \Gamma^\mu [A_\mu, \psi] \right), \quad (5.1)$$

where $A_\mu (\mu = 1, \dots, 10)$ and $\psi^\alpha (\alpha = 1, \dots, 16)$ are all $N \times N$ hermitian matrices transforming as a vector and a left-handed spinor representation under $\text{SO}(10)$. The symmetries of IIB matrix model are the matrix rotation $U(N)$, ten dimensional Lorentz symmetry $\text{SO}(10)$ and the type IIB supersymmetry. As discussed in [10], the distribution of the eigenvalues of A_μ is interpreted as the space-time itself.

It is difficult to integrate this action exactly. So we apply the IMFA by adding and subtracting a quadratic term. We specify the full propagators for bosons and fermions instead of the quadratic term S_0 . Now we focus on the dimensionality of space-time or the ratio between ‘‘our’’ space and the ‘‘internal’’ one, and consider such ansatz that the $U(N)$ symmetry remains unbroken. So gauge indices are set to preserve the $U(N)$ symmetry.

$$\langle A_\mu^i{}_j A_\nu^k{}_l \rangle = g_0^2 C_{(\mu\nu)} \delta_l^i \delta_j^k, \quad (5.2)$$

$$\langle \psi^\alpha{}^i{}_j \psi^\beta{}^k{}_l \rangle = g_0^2 \frac{i}{3!} u_{[\mu\nu\rho]} (\Gamma^{\mu\nu\rho} \mathcal{C}^{-1})^{\alpha\beta} \delta_l^i \delta_j^k, \quad (5.3)$$

where \mathcal{C} is the charge conjugation matrix such that

$${}^t\mathcal{C} = -\mathcal{C}, \quad \mathcal{C}\Gamma^\mu = -{}^t\Gamma^\mu\mathcal{C} \quad (\mu = 1, \dots, 10). \quad (5.4)$$

Since the $U(N)$ index part is symmetric in each propagator, the Lorentz index part is forced to be symmetric for bosons and anti-symmetric for fermions. We have converted the spinor indices α, β to the rank three anti-symmetric tensor $u_{[\mu\nu\rho]}$ through the gamma matrices, which is equivalent to the antisymmetric product of two left-handed spinor representations.

Here we give an overview. First, we calculate the 2PI free energy G by evaluating planar vacuum diagrams with the above exact propagators. We consider the large- N limit with the 't Hooft coupling $g = g_0^2 N$ fixed to 1. We use this g as the formal expansion parameter in the ITE later. Secondly, in order to investigate in what shape the eigenvalues distribute and to compare the free energies of various vacua we try various ansatz with symmetries which are subgroups of $\text{SO}(10)$. With these symmetries we can restrict the form of the propagators and

reduce the number of variational parameters. Thirdly, for each ansatz we make the inverse Legendre transformation to the 2PI free energy G to get the ordinary free energy F . We further apply the ITE with respect to the conjugate parameters of C and u as in eq. (4.12) and obtain the improved free energy F^{improved} . Finally, in each ansatz we extremize F^{improved} and compute the extent of the space-time from $\langle \text{Tr} (A_\mu A_\nu) \rangle$.

5.2 2PI free energy

We calculate the 2PI free energy G to the fifth order. The Feynman rules and all graphs with their symmetry factors are shown in appendices D and E. At a glance we notice that the number of graphs are much reduced by the condition of 2PI. For example, at the third order there are only four 2PI graphs as in appendix E.3, although thirty four connected graphs contribute to the ordinary free energy.

The general form of the 2PI free energy is given by²

$$\frac{G(C, u)}{N^2} = 3(1 + \log 2) - \frac{1}{2} \text{tr} \log C + \frac{1}{2} \text{tr} \log \psi - \frac{g}{2} (\text{tr} C^2 - (\text{tr} C)^2 + \text{tr}(\psi \Gamma^\mu \psi \Gamma^\nu) C_{\mu\nu}) + \dots, \quad (5.5)$$

where $\psi^\alpha_\beta = u_{\mu\nu\rho} (\Gamma^{\mu\nu\rho})^\alpha_\beta / 3!$ and the traces are taken in the vector representation for C 's and in the left-handed spinor representation for ψ 's. Although we can write down the higher order terms without evaluating the traces as in eq. (5.5), it is technically difficult to evaluate these traces and obtain a concise expression of G . Instead we evaluate the traces for each ansatz. We present in appendix G the explicit forms of G to the fifth order for the SO(7) and the SO(4) ansatz which are explained in the next subsection.

5.3 symmetries and ansatz

The guideline of making the ansatz is as follows:

- First of all, we fix a subgroup of SO(10) from SO(7) to SO(1), which will be interpreted as the rotational symmetry of “our” space-time. The component of the fermion two-point function u is non-zero only when no indices are along “our” space-time by this symmetry. In fact, we shall see that the extent of “our” space is larger than that of the remaining “internal” space.

²We adjust an additive constant to the definition of [11].

- Because u is a rank three anti-symmetric tensor, we decompose the internal space into the sum of three dimensional spaces and the rest, e.g. $4=3+1$ or $8=3+3+2$. We then assume the rotational symmetry for each space, e.g. $\text{SO}(3)\times\text{SO}(1)$ or $\text{SO}(3)\times\text{SO}(3)\times\text{SO}(2)$. This symmetry forces the component of u to be zero unless all three indices lie in one of the three dimensional spaces.
- Finally, we impose the permutation symmetry on the internal three dimensional spaces.

In this procedure, it is very important to include all parameters permitted by the imposed symmetry. Even if the free energy has an extremum in a randomly restricted parameter space, it need not be a real one in the full parameter space. On the other hand if we restrict the parameters by a symmetry, the free energy is promised to be stationary in the directions of the parameters which break the symmetry.

SO(7) ansatz

The fermion propagator is represented by the rank three anti-symmetric tensor u . Therefore if we give a non-zero value to only one element of u , $\text{SO}(10)$ symmetry breaks down to $\text{SO}(7)\times\text{SO}(3)$. Under this symmetry group, propagators are represented by three parameters, V_1, V_2, u .

$$C_{\mu\nu} = \frac{7}{8} \left(\begin{array}{ccc|ccc} 1 & & & & & \\ \vdots & & & & & \\ & & \ddots & & & \\ & & & V_1 & & \\ \hline & & & & V_2 & \\ & & & & & \ddots \\ & & & & & & V_2 \end{array} \right), \quad (5.6)$$

$$\psi = u\Gamma^{8,9,10}. \quad (5.7)$$

SO(6) ansatz

Next, we consider the case where $\text{SO}(6)$ symmetry survives. $u_{[\mu\nu\rho]}$ has non-zero values only in the extra four dimensional space. A tensor $u_{\mu\nu\rho}$ of $\text{SO}(4)$ is dual to a vector \tilde{u}^μ . Therefore up to $\text{SO}(4)$ rotation, all configurations are identical. As a result $\text{SO}(3) \subset \text{SO}(4)$ transverse to

We decompose the extra 7 dimensions to 3+3+1 , and impose $\text{SO}(3)\times\text{SO}(3)\times Z_2$ symmetry. The fermion propagator is the same as the above case. This ansatz has $\text{SO}(3)\times\text{SO}(3)\times\text{SO}(3)\times Z_2$ symmetry.

$$C_{\mu\nu} = \text{diag}(\text{three } V_1\text{'s, one } V_2, \text{ six } V_3\text{'s}), \quad (5.14)$$

$$\psi = \frac{1}{\sqrt{2}}u (\Gamma^{5,6,7} + \Gamma^{8,9,10}). \quad (5.15)$$

In the first $\text{SO}(3)$ factor (which will be interpreted as “our” space-time), the reversion of 1st direction included in Z_2 forbids the non-zero value of $u_{1,2,3}$.

SO(2) ansatz

We decompose the extra 8 dimensions to 2+3+3 , and impose $\text{SO}(2)\times\text{SO}(2)\times\text{SO}(3)\times\text{SO}(3)\times Z_2$ symmetry. We then have the following form:

$$C_{\mu\nu} = \text{diag}(\text{two } V_1\text{'s, two } V_2\text{'s, six } V_3\text{'s}), \quad (5.16)$$

$$\psi = \frac{1}{\sqrt{2}}u (\Gamma^{5,6,7} + \Gamma^{8,9,10}). \quad (5.17)$$

SO(1) ansatz³

Finally we consider the one dimensional space-time. We divide nine extra directions into three parts each of which has three dimensions. Three $\text{SO}(3)$ symmetries and permutation S_3 of these factors are imposed. S_3 is combined with the reversion of the 1st direction in order to be a subgroup of the original $\text{SO}(10)$. This ansatz has $\text{SO}(3)\times\text{SO}(3)\times\text{SO}(3)\times S_3$ symmetry.

$$C_{\mu\nu} = \text{diag}(\text{one } V_1, \text{ nine } V_2\text{'s}), \quad (5.18)$$

$$\psi = \frac{1}{\sqrt{3}}u (\Gamma^{2,3,4} + \Gamma^{5,6,7} + \Gamma^{8,9,10}). \quad (5.19)$$

5.4 free energy

The ansatz listed above have three or four parameters. Namely the boson propagator has two or three parameters V_i and the fermion propagator has one parameter u . After substituting each ansatz into the general expression of G as eq. (5.5), we obtain the 2PI free energy $G(V_i, u)$. The explicit forms of $G(V_i, u)$ are given in appendix G for the $\text{SO}(7)$ and the $\text{SO}(4)$ ansatz. As we discuss later, these cases turn out to be of particular importance. Then we make the inverse

³We use the term $\text{SO}(1)$ to indicate one dimensional space-time.

Legendre transformation to $G(V_i, u)$ in the following way. We define conjugate variables to V_i and u as

$$M^i = \frac{\partial}{\partial V_i} G(V, u), \quad (5.20)$$

$$m = \frac{\partial}{\partial u} G(V, u). \quad (5.21)$$

The ordinary free energy F is

$$F(M^i, m) = G - \sum_i M^i V_i - mu. \quad (5.22)$$

Then we apply the ITE to $F(M^i, m)$:

$$F_k^{\text{improved}}(M^i, m; M_0^i, m_0) = F(M_0^i + g(M^i - M_0^i), m_0 + g(m - m_0)) \Big|_k. \quad (5.23)$$

Here $|_k$ denotes expanding with respect to g , neglecting $O(g^{k+1})$ terms and setting $g = 1$ as in eq. (3.5). Since the action of IIB matrix model does not have a mass term, the improved free energy is given by

$$F_k^{\text{improved}}(0, 0; M_0^i, m_0) = F(M_0^i - gM_0^i, m_0 - gm_0) \Big|_k. \quad (5.24)$$

The explicit forms of $F(M_0^i - gM_0^i, m_0 - gm_0)$ for the SO(7) and the SO(4) ansatz are given in appendix H . We differentiate this free energy with respect to each parameter and set the results to zero. By solving these equations we get the extrema of the improved free energy. If there are more than one solutions, we select the one which gives the smallest free energy among them. Such a solution is expected to be on the plateau.

Fig.6 shows the free energies for the SO(7) and the SO(4) ansatz. As we explain below, the other cases are reduced to these two cases. Their numerical values are shown in Table 1. The corresponding values of M_0^i and m_0 are shown in appendix I. We find that the contribution of the fifth order is smaller than that of the third order. This fact suggests that the IMFA works well, and we can trust these results as in the case of the ϕ^4 toy model.

Some comments are in order.

- At the 2nd and the 4th order there is no reasonable extremum. As in the case of the ϕ^4 model, extrema do not necessarily appear in the even and lower order levels. Therefore we consider only the odd orders.

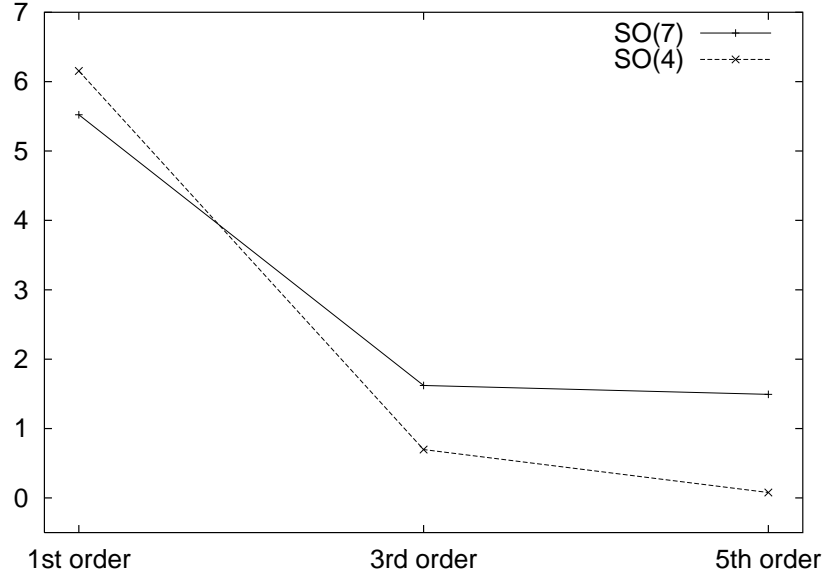


Figure 6: Free energies.

ansatz	quantities	1st order	3rd order	5th order
SO(7)	F	5.522722156	1.620942535	1.492429842
	R	0.6407423748	0.7670244718	0.8051803940
	r	0.3276944430	0.3556261073	0.3844627899
	ρ	1.955304364	2.156828390	2.094299930
SO(4)	F	6.153347114	0.696885300	0.077693647
	R	0.7500535231	1.161504610	1.7090706440
	r	0.4038451083	0.3796625830	0.2691460598
	ρ	1.857280202	3.059307619	6.349974602

Table 1: Numerical values.

- For the SO(6) ansatz, the extremum solution reduces to that of the SO(7) ansatz, i.e. V_1 and V_2 in eq. (5.8) take the same value and the SO(6) symmetry is enhanced to SO(7). In the same way the SO(5) ansatz reduces to the SO(7) ansatz. This is natural because the fermion propagators have the same form in these cases. On the other hand the SO(3) and the SO(2) ansatz reduce to the SO(4) ansatz. We thus conclude that the fermions play a crucial role in the process of the spontaneous breakdown of SO(10).
- The SO(1) ansatz has no solution even at the 1st and the 3rd order. This may indicate that one dimensional space is not realized as “our” space.

5.5 extent of space-time

Next, let us consider the extent of “our” space-time R and that of the “internal” space r . Here, for both the SO(7) and the SO(4) ansatz, R and r are defined by

$$R^2 = \left\langle \frac{1}{N} \text{Tr} A_1^2 \right\rangle = -\frac{\partial F(M^i, m)}{\partial M^1}, \quad (5.25)$$

$$r^2 = \left\langle \frac{1}{N} \text{Tr} A_{10}^2 \right\rangle = -\frac{\partial F(M^i, m)}{\partial M^2}. \quad (5.26)$$

These quantities can be also improved by the ITE, and obtained as in eq. (5.24):

$$\left\langle \frac{1}{N} \text{Tr} A_1^2 \right\rangle_k = -\frac{\partial F}{\partial M^1}(M_0^i - gM_0^i, m_0 - gm_0) \Big|_k, \quad (5.27)$$

$$\left\langle \frac{1}{N} \text{Tr} A_{10}^2 \right\rangle_k = -\frac{\partial F}{\partial M^2}(M_0^i - gM_0^i, m_0 - gm_0) \Big|_k. \quad (5.28)$$

We evaluate these quantities using the values of M_0^i and m_0 given in appendix I. R and r are shown in Fig.7, and their ratio $\rho = R/r$ is plotted in Fig.8.

In contrast to the stability of the free energy, both R and r for the SO(4) ansatz changes considerably. It is striking that their ratio grows rapidly as we increase the order of the approximation.

The fact that the SO(4) ansatz gives the lowest free energy and the large value of the extent ratio indicates that the path integral of IIB matrix model is dominated by the nearly four dimensional distribution of the eigenvalues.

6 Conclusions and discussions

Our main results are the following:

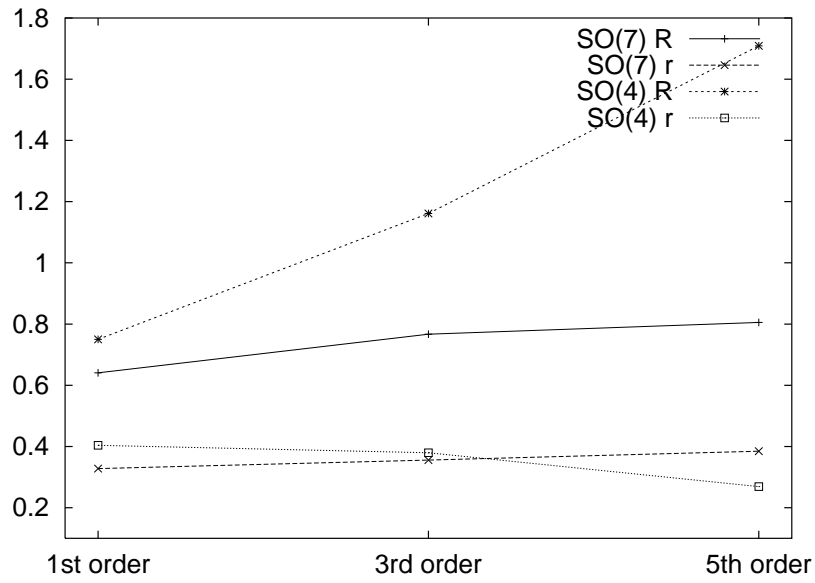


Figure 7: Extent of the space-time.

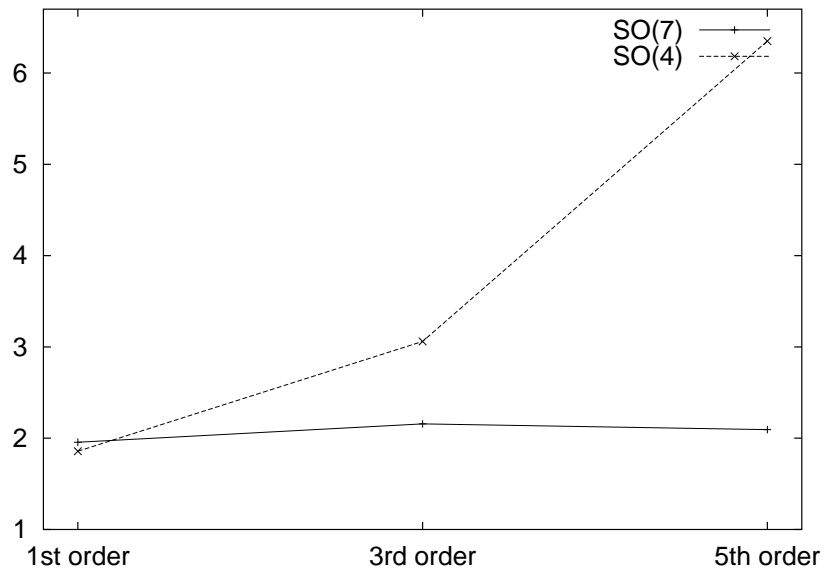


Figure 8: Ratio between the extent of "our" space-time and that of the "internal" space.

- Four dimensional configurations dominate in the path integral of IIB matrix model.
- The fermionic field plays an important role in the breakdown of the Lorentz symmetry. Its two point function seems to determine the remaining symmetry.
- For the $SO(7)$ ansatz, the free energy and the extent ratio become stable at the 5th order. On the other hand, for the $SO(4)$ ansatz, the free energy still decreases at the 5th order, but it seems to approach to a definite value. On the other hand the ratio grows more rapidly as expected. Stability of the result requires still higher order analysis.

The IMFA is, in a rigorous sense, not an “approximation” scheme. We do not know the true reason why a free energy converges to its exact value. But if we apply the IMFA to some models, the results are magically nice. To find a trick behind the IMFA should be very important.

In any ansatz except the $SO(1)$, the “internal” space shrinks in such directions that the fermion full propagator has non-zero value. We need to understand this phenomenon, shrinking by fermion, at least qualitatively. From this point of view, it would be interesting to clarify the relation between our result and the mechanism of the symmetry breaking by the phase of the fermion determinant suggested in [15].

In relation to the above connection between the “compactification” of the space and the fermion full propagator, we make a brief comment on a possibility that the full $SO(10)$ symmetry will be restored. One might wonder that eigenvalue distribution having the full $SO(10)$ symmetry is likely to be realized. However, as far as our approximation scheme is concerned, such distribution corresponds to setting all of the components of u to be zero, in which both the ordinary free energy and the 2PI free energy apparently diverge logarithmically. Therefore, it cannot be a minimum energy configuration or a solution to the SDE. This is consistent with the results in [15].

Growth of the extent ratio for the $SO(4)$ ansatz is quite interesting. To what value will it reach as going to the higher order, infinite or finite? If it is approaching infinity, we can regard it as an indication that the space-time is spontaneously compactified to the four dimensional flat space.

At any rate, the IMFA partly grasps the non-perturbative dynamics of string theory. We have extracted information on the dimension of the space-time as the first step. Probably the next step is to predict the gauge symmetry. Although some refinement to the IMFA is required, we will become able to achieve it in the near future.

There may be some directions to refine the IMFA.

- Not only two point functions but three or more point functions can be included to the SDE. Also it may be interesting to include one-point functions.
- In the present paper, we have used the 2PI free energy and the full propagators just as a calculational technique to reduce the number of graphs. But the notion of the full propagators, which has a direct connection with the SDE, may be more powerful in examining various aspects of the non-perturbative dynamics. In light of this, it would be important to investigate a direct application of the ITE to the 2PI free energy as done in appendix C.

Although there remain many unknown or ambiguous problems such as the existence of gravity, chiral fermions, the connection with the low energy effective field theory and so on, we hope we can proceed step by step with this new method.

Acknowledgments

The authors would like to thank T. Azuma, J. Nishimura, F. Sugino and T. Yokono for valuable discussions and useful comments. This work is supported in part by Grant-in-Aid for Scientific Research from Ministry of Education, Science, Sports and Culture of Japan (#1640290, #03603, #02846, #01794 and #03529). The work of T. K., T. M., S. K. and S. S. is supported in part by the Japan Society for the Promotion of Science under the Post- and Pre-doctoral Research Program.

A Some curious behavior of ITE

In sec.3, we apply the ITE to the series $\sum(-)^n x^n$. The value at $x = 3/2$ is well approximated. The method in sec.3, however, is not effective when we are to evaluate the series farther from $x = 1$. Therefore we use the ITE in a different way. The function we consider is

$$f(x) = \sum_{n=0}^{\infty} g^n (-)^n x^n (= \frac{1}{1+gx}), \quad (\text{A.1})$$

$$f_k(x) = f(x)|_k. \quad (\text{A.2})$$

As x becomes large, the behavior of the power series in x would be worse. In such a case, a more proper variable is the inverse of x , and we apply the ITE to it, i.e.

$$\frac{1}{x} \rightarrow \frac{1}{x_0} + g \left(\frac{1}{x} - \frac{1}{x_0} \right), \tag{A.3}$$

$$f_k^{\text{improved}} = f \left(\frac{1}{\frac{1}{x_0} + g \left(\frac{1}{x} - \frac{1}{x_0} \right)} \right) \Big|_k. \tag{A.4}$$

The original series of $f(x)$ without the ITE behave as shown in Fig.3.

After applying the ITE, the behavior changes drastically. Fig.9 shows the improved series at $x_0 = 0.8$. The improved series behaves well in the region $x > 1$ in which the origi-

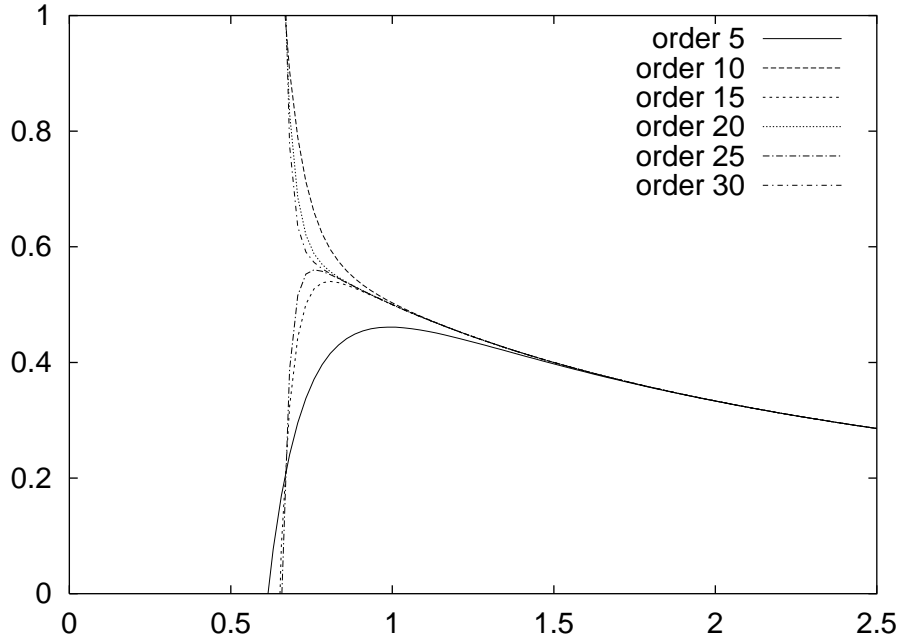


Figure 9: Improved series. The horizontal axis is x .

nal series diverges. For example, if we evaluate the value at $x = 3$, the error⁴ is almost $10^{-(\text{order of approximation})}$.

⁴Error is defined here as $\frac{(\text{approximated value}) - (\text{exact value})}{(\text{exact value})}$.

B Improved Taylor expansion for asymptotic series

Although our actual interest is in analyzing IIB matrix model and its planar sum has a finite convergence radius, ITE can also be applied to asymptotic series. We have already seen in sec.2 that the IMFA for the ϕ^4 model works well. The expansion in g of this model is only asymptotic and not convergent. As another example, we apply the ITE to Γ function here.

$$J(x) = x^{-1/2} \left(\log \Gamma(x^{-1/2}) - x^{-1/2}(\log x^{-1/2} - 1) + \frac{1}{2} \log \frac{x^{-1/2}}{2\pi} \right) \quad (\text{B.1})$$

$$= \frac{1}{12} - \frac{1}{360}gx + \frac{1}{1260}g^2x^2 - \frac{1}{1680}g^3x^3 + \frac{1}{1188}g^4x^4 - \frac{691}{360360}g^5x^5 \dots, \quad (\text{B.2})$$

which is also an asymptotic series. As in the above example, we apply the ITE for the inverse variable. Figs.10 and 11 show respectively the truncated functions without improvement and with the ITE around $x_0 = 0.03$. The behavior in the large x region is smoothed out after

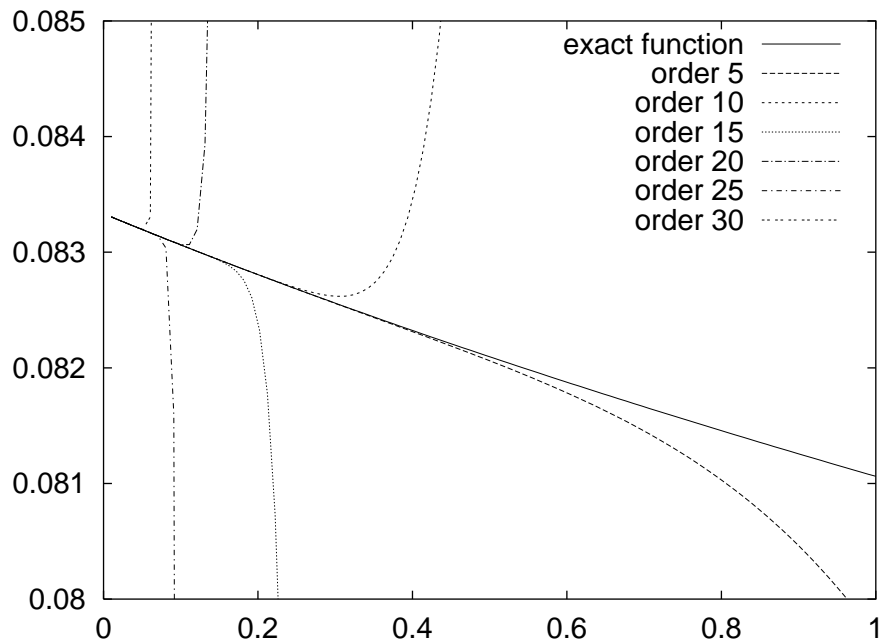


Figure 10: Original truncated functions. The horizontal axis is x .

the ITE. If we fix x to $1/3$, conversely, there is a plateau for each improved function as shown in Fig.12. The errors from the exact values at the extremum are about 10^{-5} for the improved functions of order between 6 and 26. On the other hand the truncated functions without improvement have errors of about 10^{-4} , if the order of truncation lies between 3 and 7. As

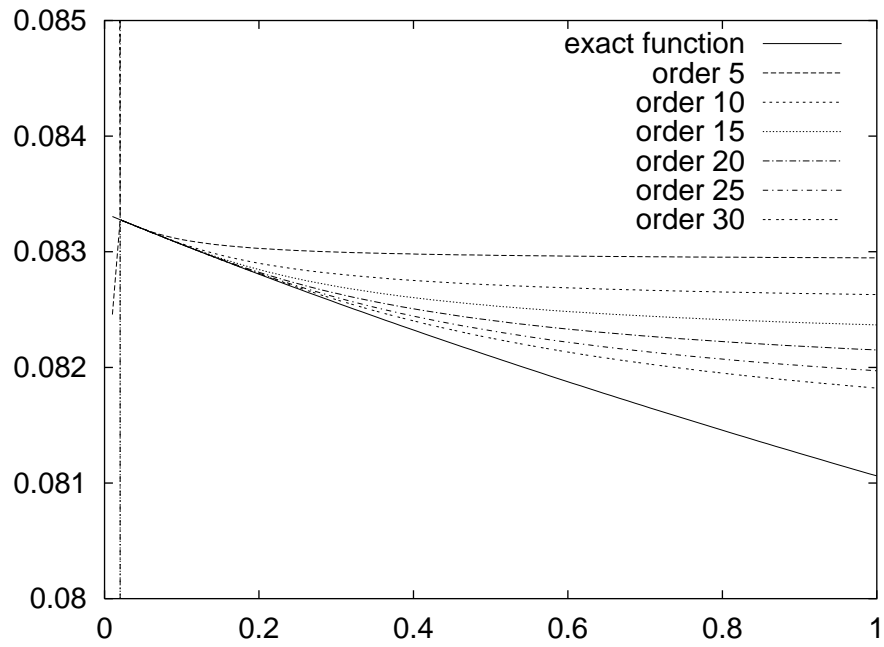


Figure 11: Improved functions. The horizontal axis is x .

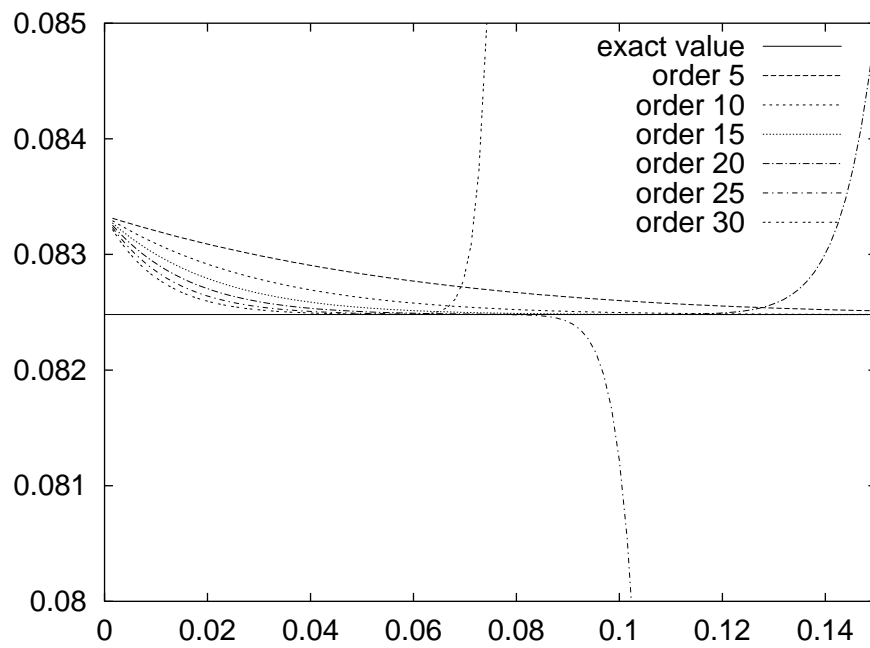


Figure 12: Plateau for each improved function. The horizontal axis is x_0 .

going to larger values of x , errors grow in both cases. At any rate the error becomes small and the oscillation becomes smooth by the ITE.

C Direct application of ITE to 2PI free energy

The ITE can be applied not only to the ordinary free energy but also to the 2PI free energy which has a direct connection to the SDE.

Let us consider the massless matrix ϕ^4 model [14].

$$S = N \frac{g^2}{4} \text{Tr} \phi^4. \quad (\text{C.1})$$

In the planar limit the perturbative expansion has a finite convergence radius. Therefore we expect that this model is more tractable than the usual ϕ^4 model.

The 2PI free energy divided by N^2 is expanded as follows :

$$G(x) = -\frac{1}{2} \log(x) + \frac{g}{2} x^2 - \frac{g^2}{8} x^4 + \frac{g^3}{6} x^6 - \frac{3g^4}{8} x^8 + \frac{11g^5}{10} x^{10} + O(g^6), \quad (\text{C.2})$$

where x is the full propagator. We can improve this function by replacing x with $x_0 + g(x - x_0)$.

If we fix x and regard G as a function of x_0 , we see a clear plateau as shown in Fig.13.

When we plot the improved 2PI free energy G by two variables x and x_0 as in Fig.14, the contour at $G = 0.4$ runs in parallel with x_0 axis at $x \sim 0.77$. Consequently, we have the plateau for x_0 and achieve a nice approximation around there. Here, in contrast to the case of the ordinary free energy, it is the full propagator x which gives the minimum of G that we are interested in, because it is nothing but a solution to the SDE. Fixing $x_0 = 0.585$ and plotting G as a function of x , we succeed to evaluate $x = 0.77$ at the minimum of G , Fig.15. This result almost reproduces the exact value $4\sqrt{3}/9 \sim 0.7698$. In this way we are able to apply the ITE directly to the 2PI free energy. There is no need for Legendre transformation, and we have more direct connection with the SDE.

D Feynman rules

We write down the Feynman rule for IIB matrix model.

- Propagators:

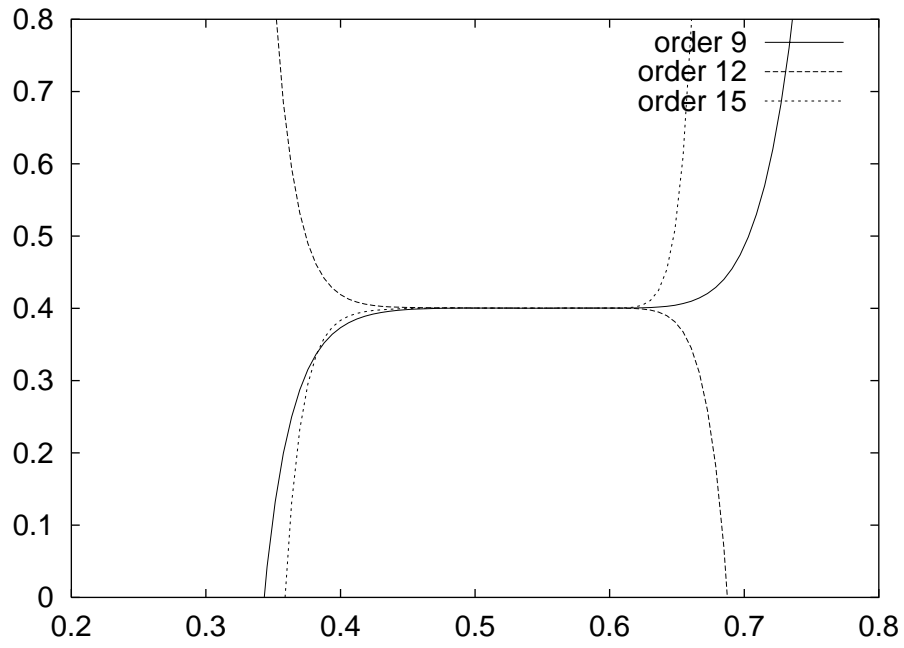


Figure 13: Plateau of improved G for $x = 0.8$. The horizontal axis is x_0 .

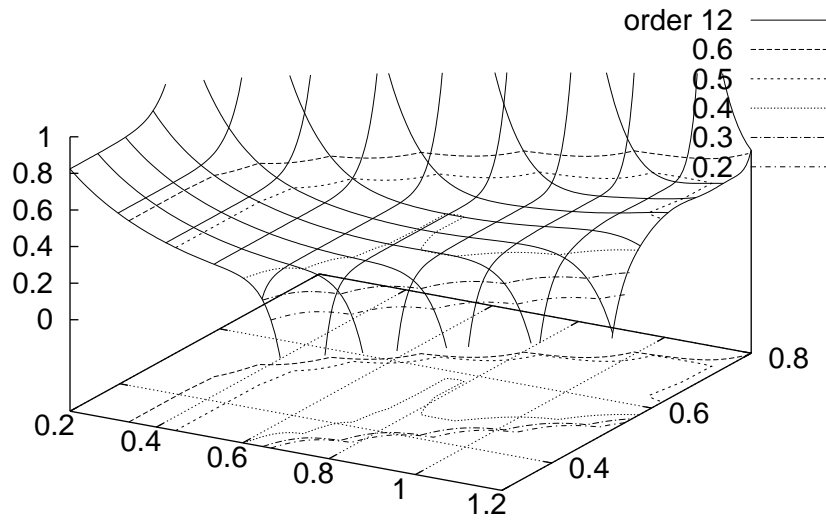


Figure 14: 3D plot of improved G at the 12th order. ($0.2 \leq x \leq 1.2$, $0.8 \leq x_0 \leq 1.2$).

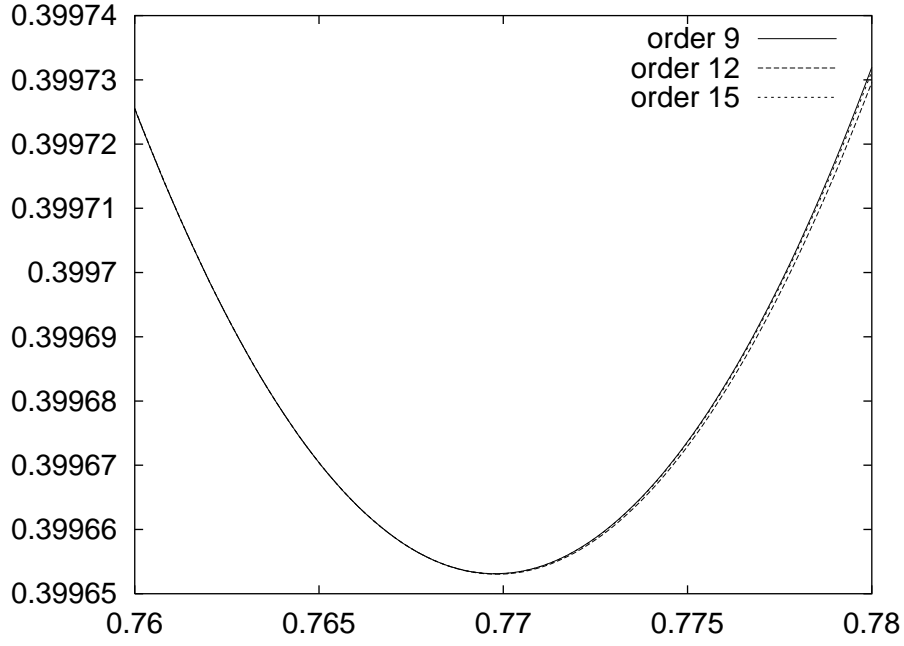


Figure 15: Minimum of improved G . The horizontal axis is x .

$$\text{-- boson : } \mu \overset{i}{\text{---}} \overset{j}{\text{---}} \nu = g_0^2 C_{\mu\nu}.$$

$$\text{-- fermion : } \alpha \overset{i}{\text{---}} \overset{j}{\text{---}} \beta = g_0^2 \frac{1}{3!} i u_{\mu\nu\rho} (\Gamma^{\mu\nu\rho} \mathcal{C}^{-1})^{\alpha\beta}.$$

• Vertices:

$$\text{-- four-boson : } \begin{array}{c} \nu \\ | \\ \mu \overset{i}{\text{---}} \overset{j}{\text{---}} \overset{l}{\text{---}} \overset{k}{\text{---}} \rho \\ | \\ \lambda \end{array} = \frac{1}{g_0^2} (2\delta^{\mu\rho}\delta^{\nu\lambda} - \delta^{\mu\nu}\delta^{\rho\lambda} - \delta^{\mu\lambda}\delta^{\nu\rho}).$$

$$\text{-- boson-fermion : } \begin{array}{c} \mu \\ | \\ \alpha \overset{i}{\text{---}} \overset{j}{\text{---}} \overset{k}{\text{---}} \beta \end{array} = \frac{1}{g_0^2} (C\Gamma^\mu)_{\alpha\beta}.$$

- Extra factors:
 - -1 for each fermion loop.
 - N for each color loop.

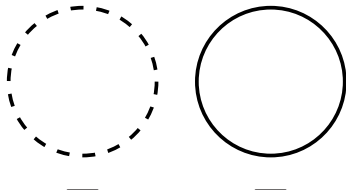
E Planar Feynman graphs

Here we show all the Feynman graphs from the zeroth order to the fifth order. The number below each graph is the symmetry factor. The value of each graph is given by

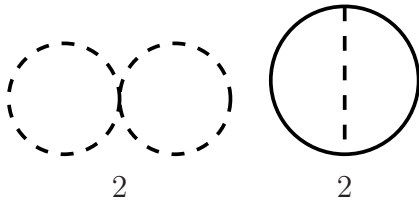
$$(-1) \times \frac{1}{\text{symmetry factor}} \times (\text{factor from Feynman rules}). \quad (\text{E.1})$$

The first factor of minus one originates from the minus sign of the definition of the free energy, $F = -\log Z$.

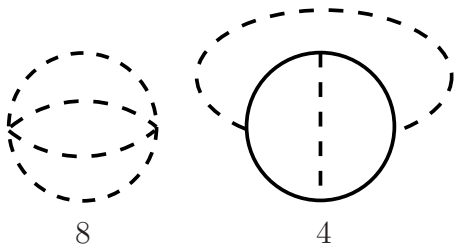
E.0 zeroth order



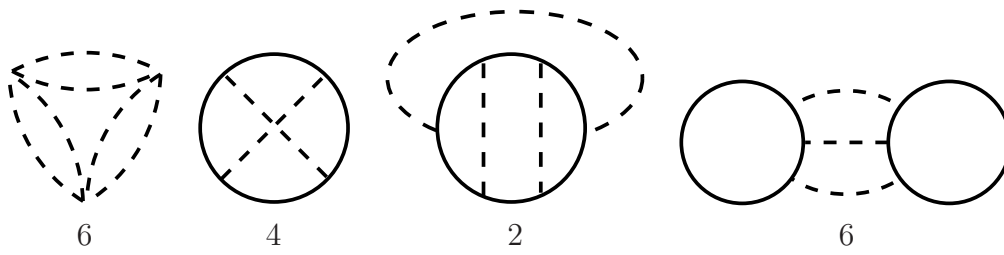
E.1 first order



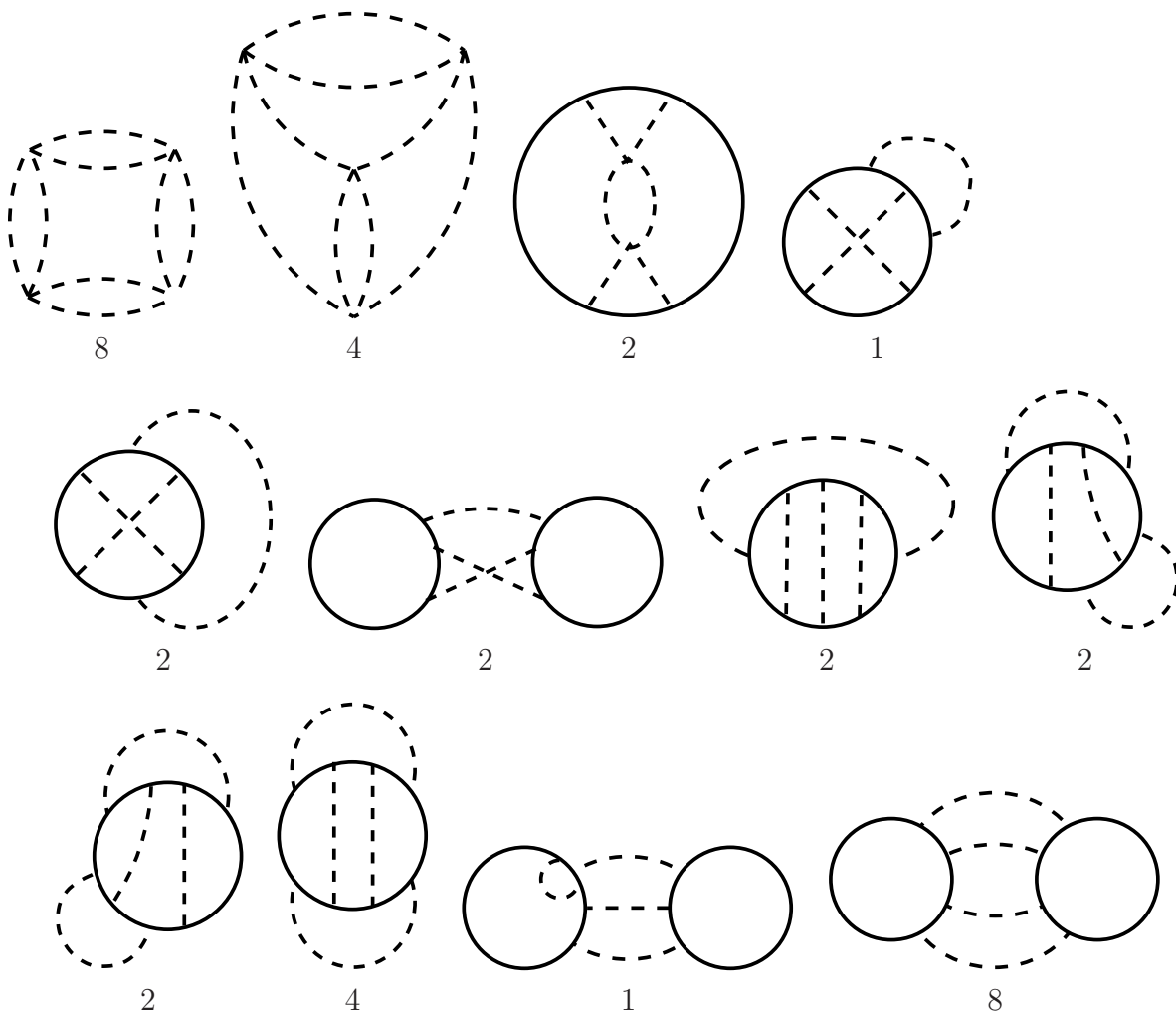
E.2 second order



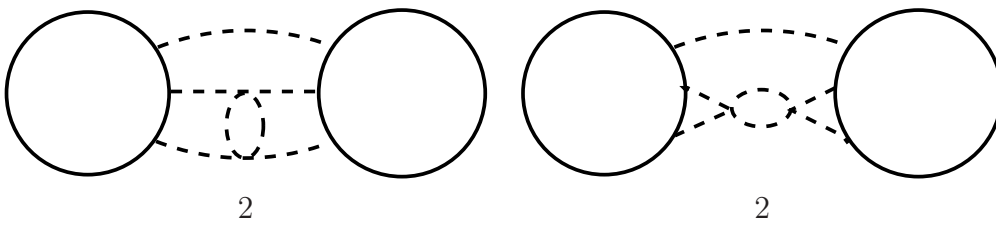
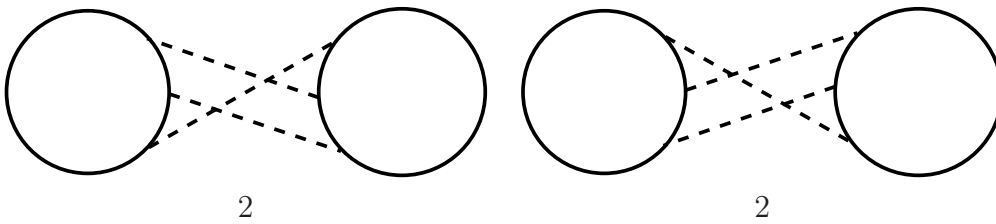
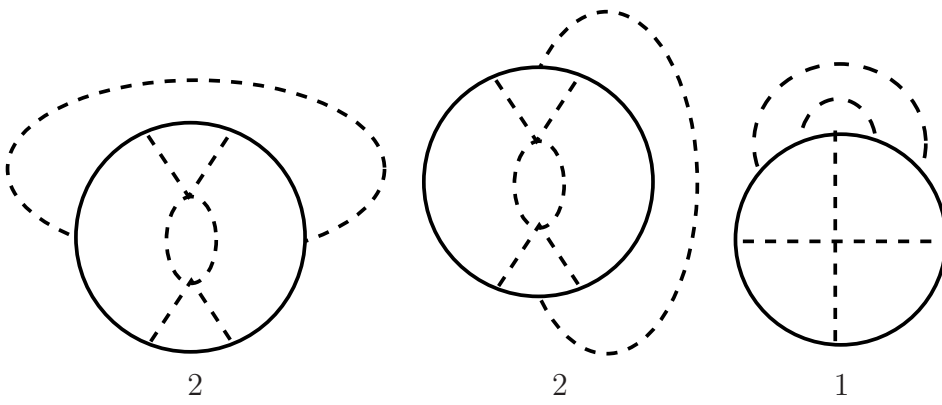
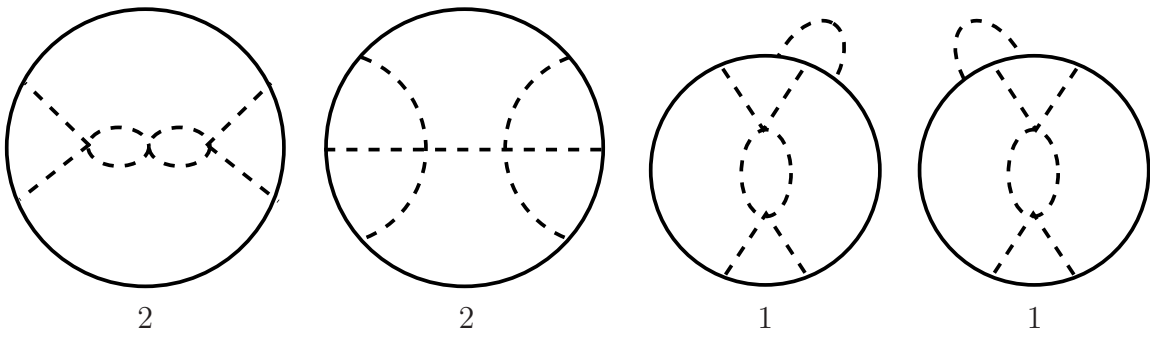
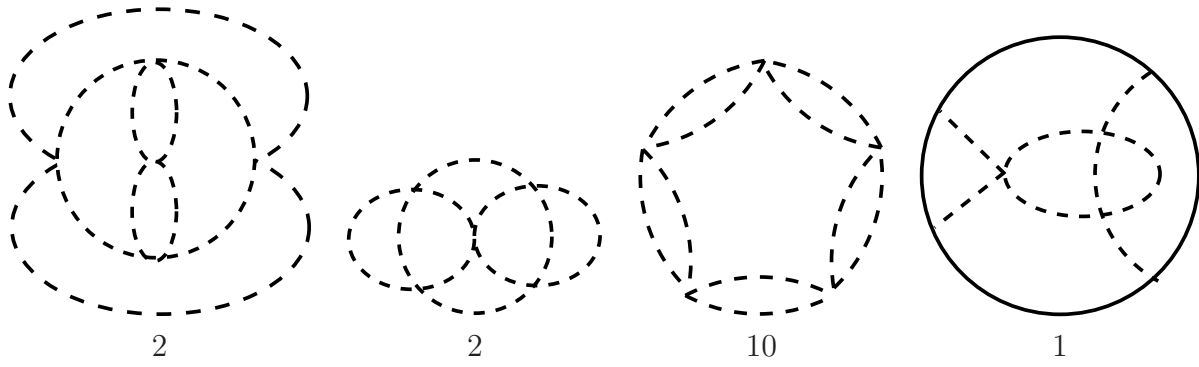
E.3 third order

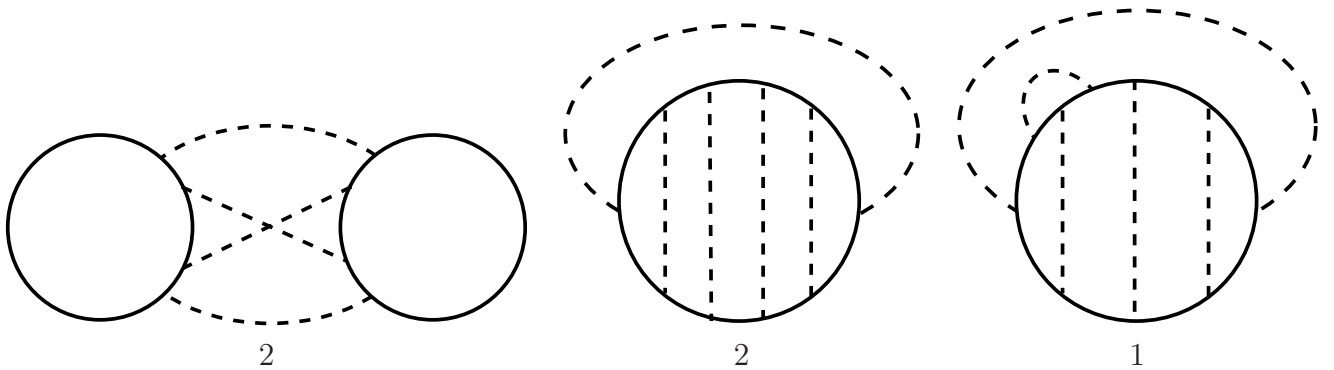
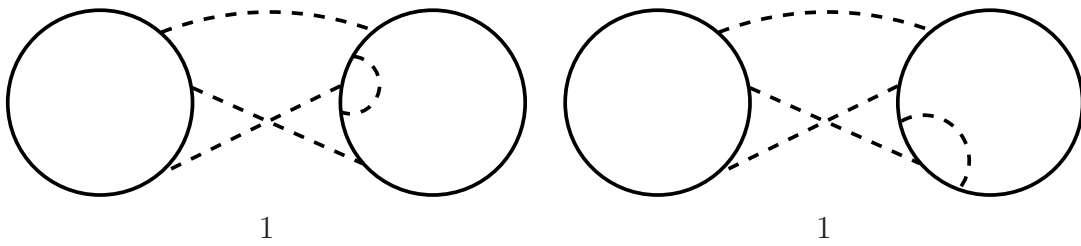
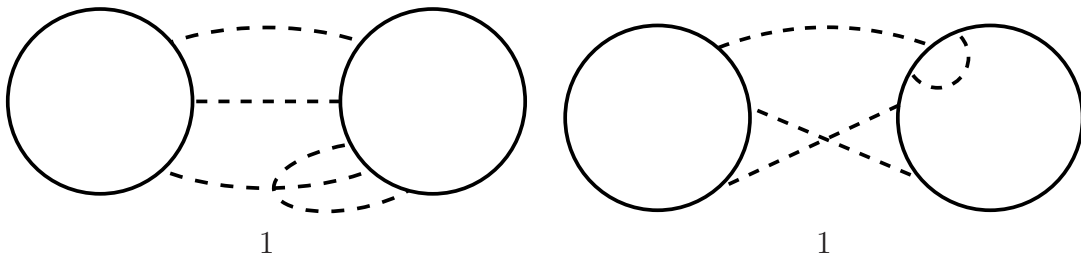
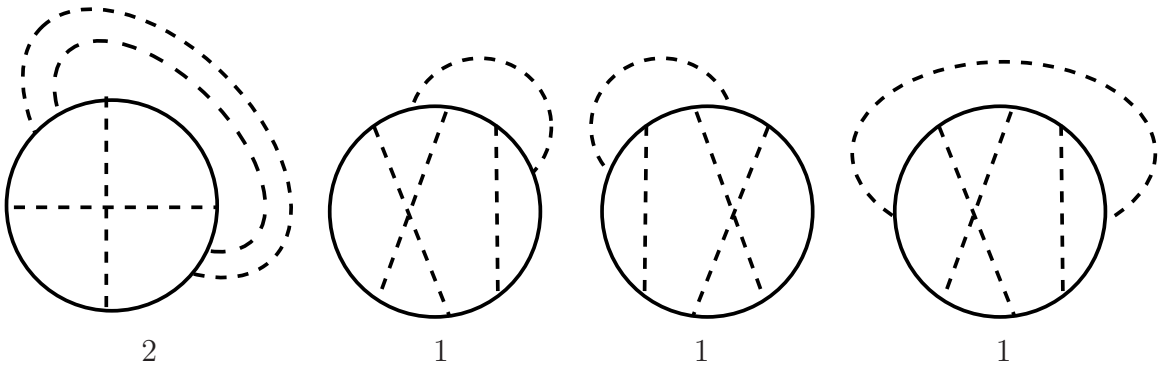
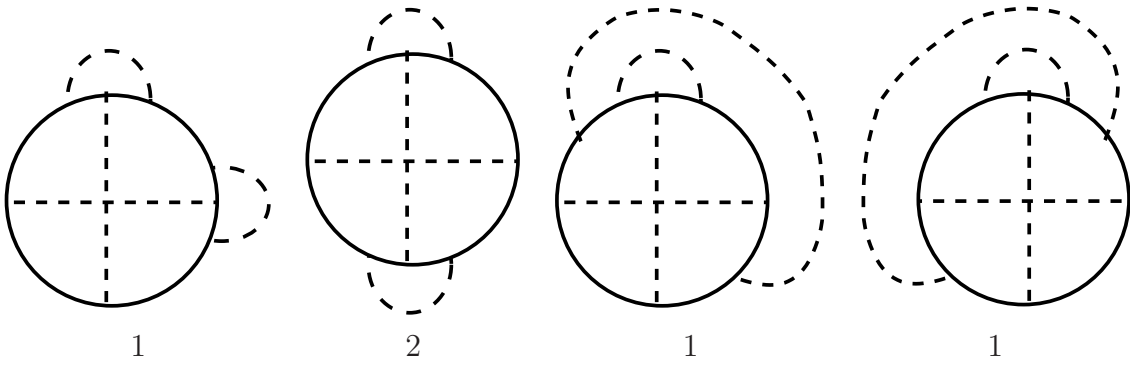


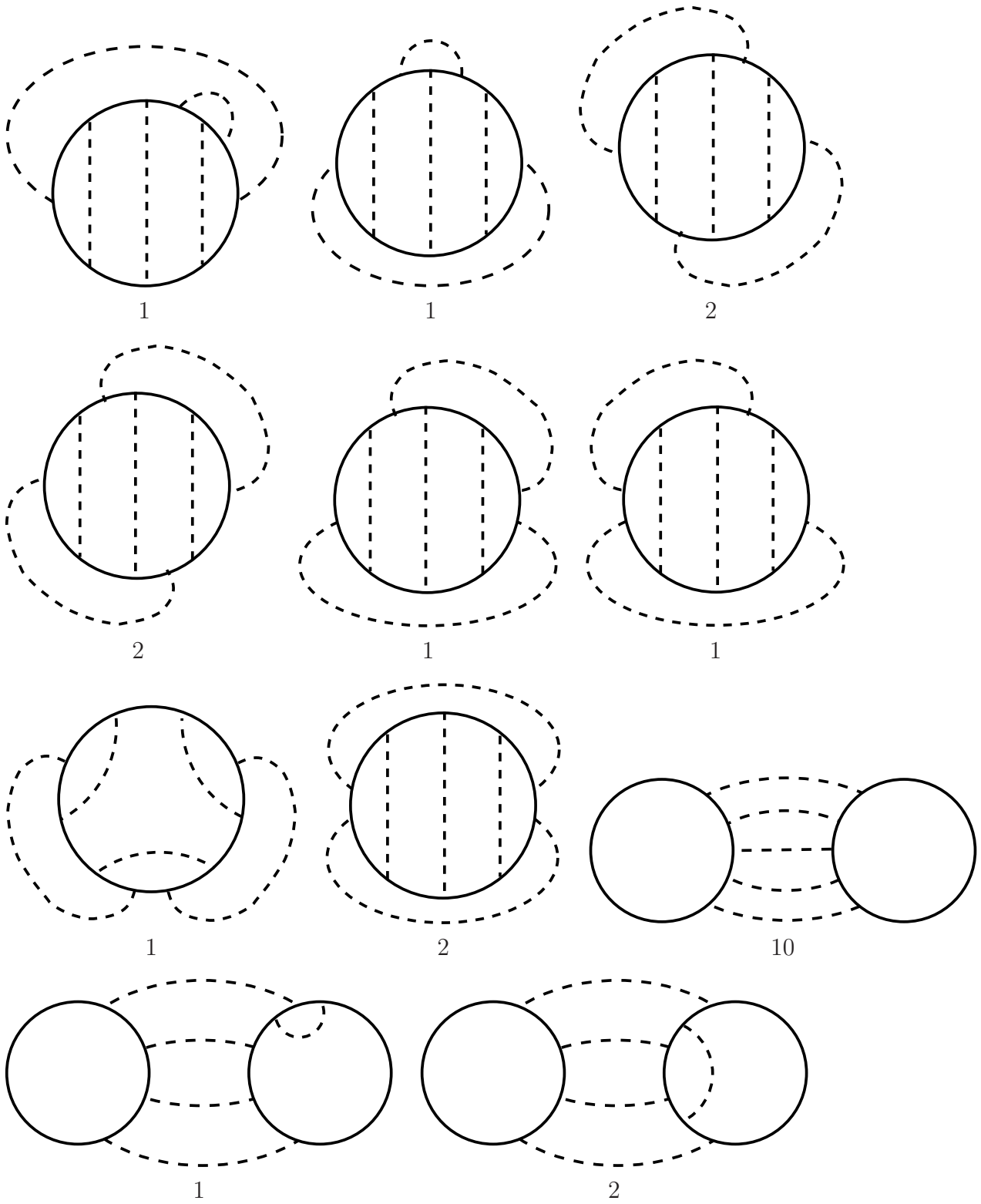
E.4 fourth order

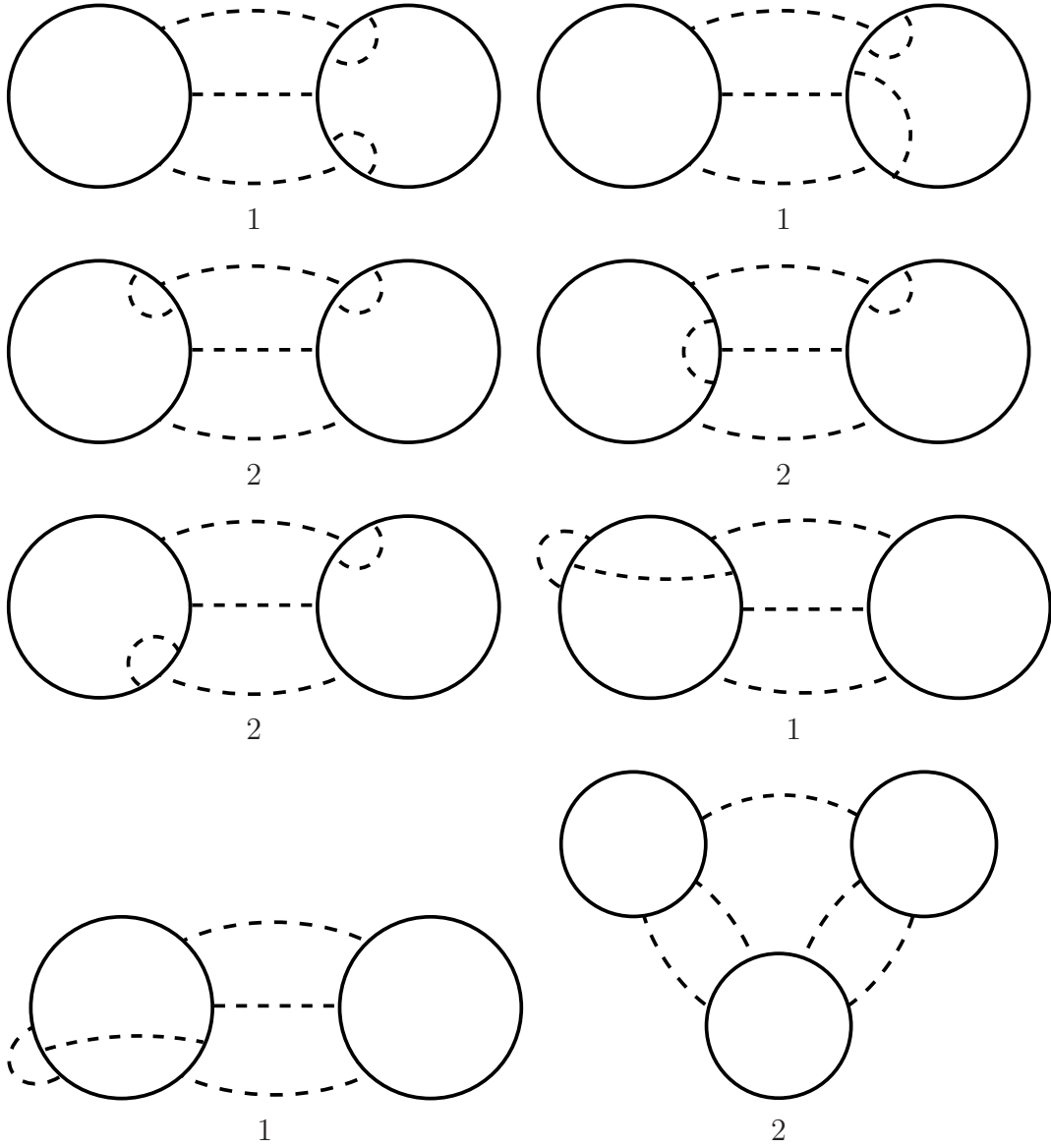


E.5 fifth order









F Derivation of SDE for full propagator

To begin with, we write the full propagator by the 1PI propagator.

$$\bullet \text{---} \square \text{---} \bullet = \bullet \text{---} \bullet + \bullet \text{---} \textcircled{\text{---}} \bullet + \bullet \text{---} \textcircled{\text{---}} \textcircled{\text{---}} \bullet + \dots \quad (\text{F.1})$$

$$= \bullet \text{---} \bullet + \bullet \text{---} \textcircled{\text{---}} \square \text{---} \bullet. \quad (\text{F.2})$$

By multiplying the inverse full propagator from the right and the inverse bare propagator from the left, we get the equation,

$$\left(\bullet \text{---} \bullet \right)^{-1} = \left(\bullet \text{---} \square \text{---} \bullet \right)^{-1} + \text{---} \textcircled{\text{---}} \text{---}. \quad (\text{F.3})$$

After combining eq.(F.3) with the relation of 1PI propagator with the full propagator,

$$\text{Full Propagator} = \text{1PI Diagram 1} + \text{1PI Diagram 2} + \dots, \quad (\text{F.4})$$

we are able to take the massless limit (set the inverse bare propagator to zero). As a result we get the eq. (4.1).

G 2PI free energy

Here we present the 2PI free energies for the SO(7) and the SO(4) ansatz.

$$\begin{aligned} \frac{G_{\text{SO}(7)}}{N^2} = & + 3 + 3 \ln(2) - \frac{1}{2} \ln(V_1^7 V_2^3) + \frac{1}{2} \ln(u^{16}) \\ & + g(21 V_1^2 + 3 V_2^2 + 21 V_1 V_2 - 56 u^2 V_1 + 24 u^2 V_2) \\ & + g^2 \left(-\frac{63}{2} V_1^4 - \frac{9}{2} V_2^4 - \frac{63}{2} V_1^2 V_2^2 - 140 u^4 V_1^2 - 168 u^4 V_1 V_2 - 12 u^4 V_2^2 \right) \\ & + g^3 (126 V_1^6 + 14 V_2^6 + 63 V_1^4 V_2^2 + 21 V_2^4 V_1^2 + 91 V_1^3 V_2^3 - 672 u^4 V_1^4 \\ & \quad - 96 u^4 V_2^4 - 1400 u^6 V_1^3 - 168 u^6 V_1 V_2^2 - 504 u^6 V_1^2 V_2 - 232 u^6 V_2^3) \\ & + g^4 (-672 V_1^4 V_2^4 - 168 V_2^6 V_1^2 - 756 V_1^6 V_2^2 - 210 V_2^5 V_1^3 - 630 V_1^5 V_2^3 - 1134 V_1^8 \\ & \quad - 75 V_2^8 - 840 u^4 V_1^4 V_2^2 - 168 u^4 V_2^4 V_1^2 - 336 u^4 V_1^3 V_2^3 + 5040 u^4 V_1^6 \\ & \quad + 528 u^4 V_2^6 - 8064 u^6 V_1^5 + 2688 u^6 V_2^5 + 9744 u^8 V_1 V_2^3 + 4032 u^6 V_1 V_2^4 \\ & \quad - 22372 u^8 V_1^4 - 22512 u^8 V_1^3 V_2 - 4032 u^6 V_1^3 V_2^2 + 1344 u^6 V_2^3 V_1^2 \\ & \quad + 168 u^8 V_1^2 V_2^2 - 12096 u^6 V_2 V_1^4 + 924 u^8 V_2^4) \\ & + g^5 (12096 V_1^{10} V_1 V_2^4 \\ & \quad + 8316 V_1^7 V_2^3 + \frac{70686}{5} V_1^{10} + 9072 V_2^4 V_1^6 - 24672 u^6 V_2^7 - 63504 u^4 V_1^8 \\ & \quad + 10206 V_1^8 V_2^2 + \frac{2838}{5} V_2^{10} + \frac{35196}{5} V_1^5 V_2^5 + 17856 u^{10} V_2^5 - 392000 u^{10} V_1^5 \\ & \quad + 22176 u^6 V_1^7 - 4080 u^4 V_2^8 + 1764 V_2^7 V_1^3 + 1470 V_2^8 V_1^2 + 3696 V_1^4 V_2^6 \\ & \quad + 3072 u^8 V_2^6 - 96768 u^8 V_1^6 - 5712 u^4 V_1^5 V_2^3 - 498624 u^{10} V_1^4 V_2 \\ & \quad - 279552 u^{10} V_1^3 V_2^2 - 139776 u^{10} V_1^2 V_2^3 - 22176 u^6 V_1 V_2^6 \\ & \quad + 23184 u^6 V_1^5 V_2^2 - 9744 u^6 V_2^5 V_1^2 - 24528 u^6 V_2^4 V_1^3 + 27216 u^6 V_1^4 V_2^3 \\ & \quad + 90720 u^6 V_2 V_1^6 - 96768 u^8 V_2^5 V_1 + 2016 u^4 V_1^6 V_2^2 + 11424 u^4 V_1^4 V_2^4) \end{aligned}$$

$$\begin{aligned}
& + 672 u^4 V_2^6 V_1^2 - 3024 u^4 V_2^5 V_1^3 - 64512 u^8 V_1^5 V_2 - 134400 u^8 V_1^4 V_2^2 \\
& - 86016 u^8 V_1^3 V_2^3 - 59136 u^8 V_2^4 V_1^2), \tag{G.1}
\end{aligned}$$

$$\begin{aligned}
\frac{G_{\text{SO}(4)}}{N^2} = & -\frac{1}{2} \ln(V_1^4 V_2^6) + 3 + 7 \ln(2) + \frac{1}{2} \ln\left(\frac{1}{256} u^{16}\right) \\
& + g(6 V_1^2 + 15 V_2^2 + 24 V_1 V_2 - 32 u^2 V_1) \\
& + g^2(-9 V_1^4 - \frac{45}{2} V_2^4 - 36 V_1^2 V_2^2 - 32 u^4 V_1^2 - 192 u^4 V_1 V_2 + 96 u^4 V_2^2) \\
& + g^3(30 V_1^6 + 85 V_2^6 + 36 V_1^4 V_2^2 + 60 V_2^4 V_1^2 + 104 V_1^3 V_2^3 - 192 u^4 V_1^4 \\
& - 384 u^4 V_1^2 V_2^2 + 192 u^4 V_2^4 - 128 u^6 V_1^3 - 768 u^6 V_1^2 V_2 - 1152 u^6 V_1 V_2^2 \\
& - 256 u^6 V_2^3) \\
& + g^4(-660 V_2^6 V_1^2 - 324 V_1^6 V_2^2 - 600 V_2^5 V_1^3 - 360 V_1^5 V_2^3 \\
& - 189 V_1^8 - 690 V_2^8 - 822 V_1^4 V_2^4 + 1152 u^4 V_1^6 + 768 u^4 V_1^4 V_2^2 \\
& + 1536 u^4 V_1^3 V_2^3 - 768 u^4 V_2^6 - 1152 u^6 V_1^5 - 4608 u^6 V_2 V_1^4 \\
& - 3840 u^6 V_1^3 V_2^2 - 3072 u^6 V_2^3 V_1^2 + 384 u^6 V_1 V_2^4 + 2304 u^6 V_2^5 \\
& - 8448 u^8 V_1^3 V_2 - 8448 u^8 V_1^2 V_2^2 - 16128 u^8 V_1 V_2^3 - 1792 u^8 V_1^4 \\
& + 3840 u^8 V_2^4) \\
& + g^5(-121344 u^{10} V_1 V_2^4 + 3456 V_1^7 V_2^3 + \frac{8496}{5} V_1^{10} \\
& + 6264 V_2^4 V_1^6 - 26880 u^6 V_2^7 - 10368 u^4 V_1^8 + 3240 V_1^8 V_2^2 + 7860 V_2^{10} \\
& + \frac{44544}{5} V_1^5 V_2^5 - 43008 u^{10} V_2^5 - 15872 u^{10} V_1^5 + 1152 u^6 V_1^7 + 7296 u^4 V_2^8 \\
& + 7200 V_2^7 V_1^3 + 8160 V_2^8 V_1^2 + 9480 V_1^4 V_2^6 - 84480 u^8 V_2^6 + 4608 u^8 V_1^6 \\
& - 12288 u^4 V_1^5 V_2^3 - 122880 u^{10} V_1^4 V_2 - 245760 u^{10} V_1^3 V_2^2 \\
& - 153600 u^{10} V_1^2 V_2^3 - 7296 u^6 V_1 V_2^6 - 12288 u^6 V_2^5 V_1^2 + 11520 u^6 V_2^4 V_1^3 \\
& + 20736 u^6 V_1^4 V_2^3 + 27648 u^6 V_2 V_1^6 + 102912 u^8 V_2^5 V_1 - 9216 u^4 V_1^6 V_2^2 \\
& - 12288 u^4 V_1^4 V_2^4 + 3072 u^4 V_2^6 V_1^2 - 7680 u^4 V_2^5 V_1^3 - 32256 u^8 V_1^5 V_2 \\
& - 113664 u^8 V_1^4 V_2^2 - 92160 u^8 V_1^3 V_2^3 - 49152 u^8 V_2^4 V_1^2). \tag{G.2}
\end{aligned}$$

H Improved free energy

We present $F(M_0^i - gM_0^i, m_0 - gm_0)$ for the SO(7) and the SO(4) ansatz. The F_k^{improved} for each ansatz is obtained by neglecting $O(g^{k+1})$ terms and setting $g = 1$ in the following expression. Here we use variables P_0^i and q_0 for notational simplicity, which are defined by $P_0^1 = -7/(2M_0^1)$, $P_0^2 = -3/(2M_0^2)$ and $q_0 = 8/m_0$ for the SO(7) ansatz and $P_0^1 = -2/M_0^1$,

$P_0^2 = -3/M_0^2$ and $q_0 = 8/m_0$ for the SO(4) ansatz. They represent the propagators of the mean field action S_0 .

$$\begin{aligned}
& \frac{1}{N^2} F_{\text{SO}(7)}(M_0^i - gM_0^i, m_0 - gm_0) = \\
& -\frac{1}{2} \ln((P_0^1)^7 (P_0^2)^3) + 3 \ln(2) + \frac{1}{2} \ln(q_0^{16}) \\
& + g(24 q_0^2 (P_0^2) + 3 (P_0^2)^2 + 21 (P_0^1)^2 - 56 q_0^2 (P_0^1) + 21 (P_0^2) (P_0^1) + 3) \\
& + g^2(-\frac{483}{2} (P_0^1)^2 (P_0^2)^2 + 42 (P_0^2) (P_0^1) - \frac{33}{2} (P_0^2)^4 \\
& \quad - 96 q_0^2 (P_0^2)^3 + 336 q_0^2 (P_0^1)^2 (P_0^2) - 84 (P_0^2)^3 (P_0^1) - 168 q_0^2 (P_0^1) + 42 (P_0^1)^2 + 6 (P_0^2)^2 + \frac{3}{2} \\
& \quad - 60 q_0^4 (P_0^2)^2 + 196 q_0^4 (P_0^1)^2 - \frac{567}{2} (P_0^1)^4 - 252 (P_0^1)^3 (P_0^2) + 72 q_0^2 (P_0^2) + 672 q_0^2 (P_0^1)^3 \\
& \quad - 336 q_0^2 (P_0^2)^2 (P_0^1) - 840 q_0^4 (P_0^1) (P_0^2)) \\
& + g^3(1 - 18144 q_0^2 (P_0^1)^5 + 1680 q_0^2 (P_0^1)^2 (P_0^2) + 6615 (P_0^1)^4 (P_0^2)^2 + 4032 q_0^2 (P_0^2)^4 (P_0^1) \\
& \quad - 5040 q_0^4 (P_0^1) (P_0^2) - 12096 q_0^2 (P_0^1)^4 (P_0^2) + 11424 (P_0^1)^2 (P_0^2)^2 q_0^4 + 5040 q_0^4 (P_0^2)^3 (P_0^1) \\
& \quad + 15624 q_0^6 (P_0^1)^2 (P_0^2) - 1680 q_0^2 (P_0^2)^2 (P_0^1) + 6384 q_0^2 (P_0^2)^3 (P_0^1)^2 - 3696 q_0^2 (P_0^1)^3 (P_0^2)^2 \\
& \quad - 168 q_0^6 (P_0^1) (P_0^2)^2 + 1152 q_0^4 (P_0^2)^4 + 7728 q_0^4 (P_0^1)^3 (P_0^2) + 2541 (P_0^2)^4 (P_0^1)^2 + 3976 q_0^6 (P_0^1)^3 \\
& \quad + 3360 q_0^2 (P_0^1)^3 + 5747 (P_0^1)^3 (P_0^2)^3 - 336 q_0^2 (P_0^1) + 1176 q_0^4 (P_0^1)^2 + 6804 (P_0^1)^5 (P_0^2) \\
& \quad + 63 (P_0^2) (P_0^1) - 966 (P_0^1)^2 (P_0^2)^2 + 1056 q_0^2 (P_0^2)^5 - 336 (P_0^2)^3 (P_0^1) + 144 q_0^2 (P_0^2) - 480 q_0^2 (P_0^2)^3 \\
& \quad - 360 q_0^4 (P_0^2)^2 - 1256 q_0^6 (P_0^2)^3 + 924 (P_0^1) (P_0^2)^5 - 1008 (P_0^1)^3 (P_0^2) + 166 (P_0^2)^6 + 6678 (P_0^1)^6 \\
& \quad + 9 (P_0^2)^2 - 66 (P_0^2)^4 - 1134 (P_0^1)^4 + 63 (P_0^1)^2) \\
& + g^4(64176 q_0^2 (P_0^1)^4 (P_0^2)^3 - 127008 q_0^2 (P_0^1)^5 + 314496 q_0^2 (P_0^1)^5 (P_0^2)^2 \\
& \quad - 313488 q_0^6 (P_0^1)^4 (P_0^2) + 5040 q_0^2 (P_0^1)^2 (P_0^2) + 39690 (P_0^1)^4 (P_0^2)^2 + 28224 q_0^2 (P_0^2)^4 (P_0^1) \\
& \quad - 17640 q_0^4 (P_0^1) (P_0^2) - 255528 (P_0^1)^4 (P_0^2)^2 q_0^4 - 182448 q_0^6 (P_0^1)^3 (P_0^2)^2 \\
& \quad - 191688 q_0^4 (P_0^2)^4 (P_0^1)^2 - 84672 q_0^2 (P_0^1)^4 (P_0^2) + 91392 (P_0^1)^2 (P_0^2)^2 q_0^4 + 40320 q_0^4 (P_0^2)^3 (P_0^1) \\
& \quad - 194544 q_0^2 (P_0^1)^3 (P_0^2)^4 + 140616 q_0^6 (P_0^1)^2 (P_0^2) + 108360 q_0^8 (P_0^1)^2 (P_0^2)^2 - 96642 (P_0^2)^5 (P_0^1)^3 \\
& \quad - 272160 (P_0^2) (P_0^1)^5 q_0^4 - 5040 q_0^2 (P_0^2)^2 (P_0^1) + 544320 q_0^2 (P_0^1)^6 (P_0^2) - 100212 q_0^8 (P_0^1)^4 \\
& \quad + 9744 q_0^6 (P_0^1) (P_0^2)^4 + 44688 q_0^2 (P_0^2)^3 (P_0^1)^2 - 25872 q_0^2 (P_0^1)^3 (P_0^2)^2 - 1512 q_0^6 (P_0^1) (P_0^2)^2 \\
& \quad - 13104 q_0^8 (P_0^1)^3 (P_0^2) + 169680 q_0^8 (P_0^1) (P_0^2)^3 + 9216 q_0^4 (P_0^2)^4 - 73920 q_0^2 (P_0^2)^6 (P_0^1) \\
& \quad + 61824 q_0^4 (P_0^1)^3 (P_0^2) - 101472 q_0^4 (P_0^2)^5 (P_0^1) - 261072 q_0^4 (P_0^1)^3 (P_0^2)^3 - 231840 q_0^6 (P_0^1)^5 \\
& \quad + 14220 q_0^8 (P_0^2)^4 - 109200 q_0^6 (P_0^2)^3 (P_0^1)^2 - 147840 q_0^2 (P_0^2)^5 (P_0^1)^2 + 15246 (P_0^2)^4 (P_0^1)^2 \\
& \quad + 35784 q_0^6 (P_0^1)^3 + 10080 q_0^2 (P_0^1)^3 + 34482 (P_0^1)^3 (P_0^2)^3 - 560 q_0^2 (P_0^1) - 26448 q_0^4 (P_0^2)^6
\end{aligned}$$

$$\begin{aligned}
& + 4116 q_0^4 (P_0^1)^2 - 187110 (P_0^1)^4 (P_0^2)^4 + 40824 (P_0^1)^5 (P_0^2) + 84 (P_0^2) (P_0^1) + 13920 q_0^6 (P_0^2)^5 \\
& - 2415 (P_0^1)^2 (P_0^2)^2 + 7392 q_0^2 (P_0^2)^5 - 840 (P_0^2)^3 (P_0^1) + 240 q_0^2 (P_0^2) - 1440 q_0^2 (P_0^2)^3 \\
& - 1260 q_0^4 (P_0^2)^2 - 42672 (P_0^2)^6 (P_0^1)^2 - 11304 q_0^6 (P_0^2)^3 + 5544 (P_0^1) (P_0^2)^5 - 178416 (P_0^1)^6 q_0^4 \\
& - 236502 (P_0^1)^5 (P_0^2)^3 - 240408 (P_0^1)^7 (P_0^2) + 641088 q_0^2 (P_0^1)^7 - 247212 (P_0^1)^6 (P_0^2)^2 \\
& - 13944 (P_0^2)^7 (P_0^1) - 2520 (P_0^1)^3 (P_0^2) - 15936 (P_0^2)^7 q_0^2 + 996 (P_0^2)^6 + 40068 (P_0^1)^6 + 12 (P_0^2)^2 \\
& - 165 (P_0^2)^4 - 2835 (P_0^1)^4 + 84 (P_0^1)^2 - 202986 (P_0^1)^8 - 2199 (P_0^2)^8 + \frac{3}{4} \\
& + g^5 (577584 q_0^2 (P_0^1)^4 (P_0^2)^3 - 508032 q_0^2 (P_0^1)^5 + 2830464 q_0^2 (P_0^1)^5 (P_0^2)^2 \\
& - 11009376 (P_0^1)^6 (P_0^2)^3 q_0^2 - 3448368 q_0^6 (P_0^1)^4 (P_0^2) + 11760 q_0^2 (P_0^1)^2 (P_0^2) \\
& + 1878912 q_0^6 (P_0^2)^5 (P_0^1)^2 + 138915 (P_0^1)^4 (P_0^2)^2 + 3873408 (P_0^1)^2 (P_0^2)^7 q_0^2 \\
& + 112896 q_0^2 (P_0^2)^4 (P_0^1) - 780864 q_0^8 (P_0^1)^3 (P_0^2)^3 + 8285760 q_0^4 (P_0^1)^4 (P_0^2)^4 \\
& - 47040 q_0^4 (P_0^1) (P_0^2) - 3321696 q_0^8 (P_0^2)^5 (P_0^1) - 4235616 (P_0^2) q_0^8 (P_0^1)^5 \\
& + 11690784 (P_0^1)^6 q_0^4 (P_0^2)^2 - 2555280 (P_0^1)^4 (P_0^2)^2 q_0^4 - 2006928 q_0^6 (P_0^1)^3 (P_0^2)^2 \\
& + 1561728 (P_0^2)^8 q_0^2 (P_0^1) + 9767520 (P_0^2) q_0^6 (P_0^1)^6 - 19885824 (P_0^1)^7 (P_0^2)^2 q_0^2 \\
& - 4906944 q_0^8 (P_0^1)^4 (P_0^2)^2 - 1916880 q_0^4 (P_0^2)^4 (P_0^1)^2 - 338688 q_0^2 (P_0^1)^4 (P_0^2) \\
& + 411264 (P_0^1)^2 (P_0^2)^2 q_0^4 - 6339648 q_0^8 (P_0^1)^2 (P_0^2)^4 + 181440 q_0^4 (P_0^2)^3 (P_0^1) \\
& - 622944 (P_0^1)^5 (P_0^2)^4 q_0^2 + 5608512 q_0^6 (P_0^2)^2 (P_0^1)^5 - 26925696 (P_0^2) (P_0^1)^8 q_0^2 \\
& - 1750896 q_0^2 (P_0^1)^3 (P_0^2)^4 + 703080 q_0^6 (P_0^1)^2 (P_0^2) + 16039296 (P_0^2) q_0^4 (P_0^1)^7 \\
& + 1300320 q_0^8 (P_0^1)^2 (P_0^2)^2 - 773136 (P_0^2)^5 (P_0^1)^3 - 2721600 (P_0^2) (P_0^1)^5 q_0^4 \\
& - 11760 q_0^2 (P_0^2)^2 (P_0^1) - 570528 q_0^{10} (P_0^1) (P_0^2)^4 - 8170848 (P_0^2) q_0^{10} (P_0^1)^4 \\
& + 4898880 q_0^2 (P_0^1)^6 (P_0^2) + 2779392 q_0^4 (P_0^2)^7 (P_0^1) - 1202544 q_0^8 (P_0^1)^4 \\
& + 5450592 q_0^4 (P_0^2)^6 (P_0^1)^2 + 107184 q_0^6 (P_0^1) (P_0^2)^4 + 178752 q_0^2 (P_0^2)^3 (P_0^1)^2 \\
& + 8013600 q_0^4 (P_0^1)^3 (P_0^2)^5 + 9508128 q_0^4 (P_0^1)^5 (P_0^2)^3 - 103488 q_0^2 (P_0^1)^3 (P_0^2)^2 \\
& - 7560 q_0^6 (P_0^1) (P_0^2)^2 - 157248 q_0^8 (P_0^1)^3 (P_0^2) - 1912512 q_0^{10} (P_0^1)^3 (P_0^2)^2 \\
& + 2036160 q_0^8 (P_0^1) (P_0^2)^3 + 5197920 q_0^6 (P_0^1)^3 (P_0^2)^4 + 41472 q_0^4 (P_0^2)^4 \\
& + 4110624 q_0^6 (P_0^1)^4 (P_0^2)^3 - 665280 q_0^2 (P_0^2)^6 (P_0^1) + 278208 q_0^4 (P_0^1)^3 (P_0^2) \\
& + 364896 q_0^6 (P_0^2)^6 (P_0^1) - 1014720 q_0^4 (P_0^2)^5 (P_0^1) - 2610720 q_0^4 (P_0^1)^3 (P_0^2)^3 \\
& - 2550240 q_0^6 (P_0^1)^5 - 9748032 q_0^{10} (P_0^1)^2 (P_0^2)^3 + 170640 q_0^8 (P_0^2)^4 \\
& - 1201200 q_0^6 (P_0^2)^3 (P_0^1)^2 + 7336224 (P_0^1)^4 (P_0^2)^5 q_0^2 - 1330560 q_0^2 (P_0^2)^5 (P_0^1)^2 \\
& + 53361 (P_0^2)^4 (P_0^1)^2 + 6365856 (P_0^1)^3 (P_0^2)^6 q_0^2 + 178920 q_0^6 (P_0^1)^3 + 23520 q_0^2 (P_0^1)^3 \\
& + 120687 (P_0^1)^3 (P_0^2)^3 - 840 q_0^2 (P_0^1) - 264480 q_0^4 (P_0^2)^6 + 10976 q_0^4 (P_0^1)^2
\end{aligned}$$

$$\begin{aligned}
& - 1496880 (P_0^1)^4 (P_0^2)^4 + 142884 (P_0^1)^5 (P_0^2) + 105 (P_0^2) (P_0^1) + 153120 q_0^6 (P_0^2)^5 \\
& - 4830 (P_0^1)^2 (P_0^2)^2 + 281472 (P_0^2)^9 q_0^2 + 246288 (P_0^2)^9 (P_0^1) + 29568 q_0^2 (P_0^2)^5 - 1680 (P_0^2)^3 (P_0^1) \\
& + 360 q_0^2 (P_0^2) - 3360 q_0^2 (P_0^2)^3 - 3360 q_0^4 (P_0^2)^2 - 341376 (P_0^2)^6 (P_0^1)^2 - 56520 q_0^6 (P_0^2)^3 \\
& + 19404 (P_0^1) (P_0^2)^5 - 1784160 (P_0^1)^6 q_0^4 - 1892016 (P_0^1)^5 (P_0^2)^3 - 1923264 (P_0^1)^7 (P_0^2) \\
& + 5769792 q_0^2 (P_0^1)^7 - 1977696 (P_0^1)^6 (P_0^2)^2 - 25982208 (P_0^1)^9 q_0^2 - \frac{476448}{5} q_0^{10} (P_0^1)^5 \\
& + 14270256 q_0^4 (P_0^1)^8 + 3342528 q_0^8 (P_0^1)^6 + 10644480 q_0^6 (P_0^1)^7 + 9743328 (P_0^2) (P_0^1)^9 \\
& - 111552 (P_0^2)^7 (P_0^1) - 5040 (P_0^1)^3 (P_0^2) - 143424 (P_0^2)^7 q_0^2 + 4224276 (P_0^1)^4 (P_0^2)^6 \\
& - 18432 q_0^6 (P_0^2)^7 + \frac{1239072}{5} q_0^{10} (P_0^2)^5 + 10877328 (P_0^1)^7 (P_0^2)^3 + 627792 q_0^4 (P_0^2)^8 \\
& + 10724238 (P_0^1)^8 (P_0^2)^2 + \frac{37165968}{5} (P_0^2)^5 (P_0^1)^5 + 9821196 (P_0^1)^6 (P_0^2)^4 + 2083536 (P_0^1)^3 (P_0^2)^7 \\
& - 604608 q_0^8 (P_0^2)^6 + 853230 (P_0^2)^8 (P_0^1)^2 + 3486 (P_0^2)^6 + 140238 (P_0^1)^6 + 15 (P_0^2)^2 - 330 (P_0^2)^4 \\
& - 5670 (P_0^1)^4 + 105 (P_0^1)^2 - 1623888 (P_0^1)^8 - 17592 (P_0^2)^8 + \frac{170934}{5} (P_0^2)^{10} + \frac{3}{5} \\
& + \frac{35778078}{5} (P_0^1)^{10}), \tag{H.1}
\end{aligned}$$

$$\begin{aligned}
& \frac{1}{N^2} F_{\text{SO}(4)}(M_0^i - gM_0^i, m_0 - gm_0) = \\
& 3 \ln(2) + \frac{1}{2} \ln(q_0^{16}) - \frac{1}{2} \ln((P_0^1)^4 (P_0^2)^6) \\
& + g(3 - 32 q_0^2 (P_0^1) + 6 (P_0^1)^2 + 15 (P_0^2)^2 + 24 (P_0^2) (P_0^1)) \\
& + g^2(12 (P_0^1)^2 \\
& - 240 (P_0^2)^3 (P_0^1) - 45 (P_0^1)^4 - 32 q_0^4 (P_0^1)^2 - \frac{345}{2} (P_0^2)^4 + 384 q_0^2 (P_0^1)^2 (P_0^2) + 96 q_0^4 (P_0^2)^2 \\
& - 192 q_0^4 (P_0^1) (P_0^2) + 192 q_0^2 (P_0^1)^3 + \frac{3}{2} - 276 (P_0^1)^2 (P_0^2)^2 - 144 (P_0^1)^3 (P_0^2) - 96 q_0^2 (P_0^1) \\
& + 48 (P_0^2) (P_0^1) + 30 (P_0^2)^2) \\
& + g^3(1 - 2880 q_0^2 (P_0^1)^5 + 1920 q_0^2 (P_0^1)^2 (P_0^2) + 4212 (P_0^1)^4 (P_0^2)^2 - 1152 q_0^4 (P_0^1) (P_0^2) \\
& - 6912 q_0^2 (P_0^1)^4 (P_0^2) + 3456 (P_0^1)^2 (P_0^2)^2 q_0^4 + 384 q_0^4 (P_0^2)^3 (P_0^1) + 2304 q_0^6 (P_0^1)^2 (P_0^2) \\
& - 3840 q_0^2 (P_0^2)^3 (P_0^1)^2 - 8832 q_0^2 (P_0^1)^3 (P_0^2)^2 - 4224 q_0^6 (P_0^1) (P_0^2)^2 - 1728 q_0^4 (P_0^2)^4 \\
& + 1920 q_0^4 (P_0^1)^3 (P_0^2) + 6540 (P_0^2)^4 (P_0^1)^2 + 1920 q_0^6 (P_0^1)^3 + 960 q_0^2 (P_0^1)^3 + 6952 (P_0^1)^3 (P_0^2)^3 \\
& - 192 q_0^2 (P_0^1) - 192 q_0^4 (P_0^1)^2 + 2160 (P_0^1)^5 (P_0^2) + 72 (P_0^2) (P_0^1) - 1104 (P_0^1)^2 (P_0^2)^2 \\
& - 960 (P_0^2)^3 (P_0^1) + 576 q_0^4 (P_0^2)^2 - 256 q_0^6 (P_0^2)^3 + 5520 (P_0^1) (P_0^2)^5 - 576 (P_0^1)^3 (P_0^2) + 3485 (P_0^2)^6 \\
& + 606 (P_0^1)^6 + 45 (P_0^2)^2 - 690 (P_0^2)^4 - 180 (P_0^1)^4 + 18 (P_0^1)^2 + 1728 q_0^4 (P_0^1)^4) \\
& + g^4(333696 q_0^2 (P_0^1)^4 (P_0^2)^3 - 20160 q_0^2 (P_0^1)^5 + 269568 q_0^2 (P_0^1)^5 (P_0^2)^2 - 82944 q_0^6 (P_0^1)^4 (P_0^2)
\end{aligned}$$

$$\begin{aligned}
& + 5760 q_0^2 (P_0^1)^2 (P_0^2) + 25272 (P_0^1)^4 (P_0^2)^2 - 4032 q_0^4 (P_0^1) (P_0^2) - 110592 (P_0^1)^4 (P_0^2)^2 q_0^4 \\
& - 27648 q_0^6 (P_0^1)^3 (P_0^2)^2 - 43008 q_0^4 (P_0^2)^4 (P_0^1)^2 - 48384 q_0^2 (P_0^1)^4 (P_0^2) + 27648 (P_0^1)^2 (P_0^2)^2 q_0^4 \\
& + 3072 q_0^4 (P_0^2)^3 (P_0^1) + 209280 q_0^2 (P_0^1)^3 (P_0^2)^4 + 20736 q_0^6 (P_0^1)^2 (P_0^2) + 80640 q_0^8 (P_0^1)^2 (P_0^2)^2 \\
& - 246600 (P_0^2)^5 (P_0^1)^3 - 100224 (P_0^2) (P_0^1)^5 q_0^4 + 172800 q_0^2 (P_0^1)^6 (P_0^2) + 2304 q_0^8 (P_0^1)^4 \\
& + 84864 q_0^6 (P_0^1) (P_0^2)^4 - 26880 q_0^2 (P_0^2)^3 (P_0^1)^2 - 61824 q_0^2 (P_0^1)^3 (P_0^2)^2 - 38016 q_0^6 (P_0^1) (P_0^2)^2 \\
& + 34560 q_0^8 (P_0^1)^3 (P_0^2) - 28416 q_0^8 (P_0^1) (P_0^2)^3 - 13824 q_0^4 (P_0^2)^4 + 15360 q_0^4 (P_0^1)^3 (P_0^2) \\
& + 11136 q_0^4 (P_0^2)^5 (P_0^1) - 99840 q_0^4 (P_0^1)^3 (P_0^2)^3 - 35712 q_0^6 (P_0^1)^5 + 6912 q_0^8 (P_0^2)^4 \\
& + 67584 q_0^6 (P_0^2)^3 (P_0^1)^2 + 88320 q_0^2 (P_0^2)^5 (P_0^1)^2 + 39240 (P_0^2)^4 (P_0^1)^2 + 17280 q_0^6 (P_0^1)^3 \\
& + 2880 q_0^2 (P_0^1)^3 + 41712 (P_0^1)^3 (P_0^2)^3 - 320 q_0^2 (P_0^1) + 45312 q_0^4 (P_0^2)^6 - 672 q_0^4 (P_0^1)^2 \\
& - 238374 (P_0^1)^4 (P_0^2)^4 + 12960 (P_0^1)^5 (P_0^2) + 96 (P_0^2) (P_0^1) + 9984 q_0^6 (P_0^2)^5 - 2760 (P_0^1)^2 (P_0^2)^2 \\
& - 2400 (P_0^2)^3 (P_0^1) + 2016 q_0^4 (P_0^2)^2 - 214260 (P_0^2)^6 (P_0^1)^2 - 2304 q_0^6 (P_0^2)^3 + 33120 (P_0^1) (P_0^2)^5 \\
& - 61056 (P_0^1)^6 q_0^4 - 163224 (P_0^1)^5 (P_0^2)^3 - 43632 (P_0^1)^7 (P_0^2) + 58176 q_0^2 (P_0^1)^7 + 60 (P_0^2)^2 \\
& - 94500 (P_0^1)^6 (P_0^2)^2 - 167280 (P_0^2)^7 (P_0^1) - 1440 (P_0^1)^3 (P_0^2) + 20910 (P_0^2)^6 + 3636 (P_0^1)^6 \\
& - 1725 (P_0^2)^4 - 450 (P_0^1)^4 + 24 (P_0^1)^2 - 10665 (P_0^1)^8 - 91140 (P_0^2)^8 + \frac{3}{4} + 13824 q_0^4 (P_0^1)^4 \\
& + g^5 (3003264 q_0^2 (P_0^1)^4 (P_0^2)^3 - 80640 q_0^2 (P_0^1)^5 + 2426112 q_0^2 (P_0^1)^5 (P_0^2)^2 \\
& - 13057920 (P_0^1)^6 (P_0^2)^3 q_0^2 - 912384 q_0^6 (P_0^1)^4 (P_0^2) + 13440 q_0^2 (P_0^1)^2 (P_0^2) \\
& - 2666496 q_0^6 (P_0^2)^5 (P_0^1)^2 + 88452 (P_0^1)^4 (P_0^2)^2 - 2676480 (P_0^1)^2 (P_0^2)^7 q_0^2 \\
& - 2239488 q_0^8 (P_0^1)^3 (P_0^2)^3 + 4918272 q_0^4 (P_0^1)^4 (P_0^2)^4 - 10752 q_0^4 (P_0^1) (P_0^2) \\
& + 476160 q_0^8 (P_0^2)^5 (P_0^1) - 1244160 (P_0^2) q_0^8 (P_0^1)^5 + 5985792 (P_0^1)^6 q_0^4 (P_0^2)^2 \\
& - 1105920 (P_0^1)^4 (P_0^2)^2 q_0^4 - 304128 q_0^6 (P_0^1)^3 (P_0^2)^2 + 2059776 (P_0^2) q_0^6 (P_0^1)^6 \\
& - 9072000 (P_0^1)^7 (P_0^2)^2 q_0^2 - 2276352 q_0^8 (P_0^1)^4 (P_0^2)^2 - 430080 q_0^4 (P_0^2)^4 (P_0^1)^2 \\
& - 193536 q_0^2 (P_0^1)^4 (P_0^2) + 124416 (P_0^1)^2 (P_0^2)^2 q_0^4 - 602112 q_0^8 (P_0^1)^2 (P_0^2)^4 \\
& + 13824 q_0^4 (P_0^2)^3 (P_0^1) - 15255936 (P_0^1)^5 (P_0^2)^4 q_0^2 + 2366208 q_0^6 (P_0^2)^2 (P_0^1)^5 \\
& - 4886784 (P_0^2) (P_0^1)^8 q_0^2 + 1883520 q_0^2 (P_0^1)^3 (P_0^2)^4 + 103680 q_0^6 (P_0^1)^2 (P_0^2) \\
& + 4745088 (P_0^2) q_0^4 (P_0^1)^7 + 967680 q_0^8 (P_0^1)^2 (P_0^2)^2 - 1972800 (P_0^2)^5 (P_0^1)^3 \\
& - 1002240 (P_0^2) (P_0^1)^5 q_0^4 - 723456 q_0^{10} (P_0^1) (P_0^2)^4 - 958464 (P_0^2) q_0^{10} (P_0^1)^4 \\
& + 1555200 q_0^2 (P_0^1)^6 (P_0^2) - 836736 q_0^4 (P_0^2)^7 (P_0^1) + 27648 q_0^8 (P_0^1)^4 + 663552 q_0^4 (P_0^2)^6 (P_0^1)^2 \\
& + 933504 q_0^6 (P_0^1) (P_0^2)^4 - 107520 q_0^2 (P_0^2)^3 (P_0^1)^2 + 2390016 q_0^4 (P_0^1)^3 (P_0^2)^5 \\
& + 6532608 q_0^4 (P_0^1)^5 (P_0^2)^3 - 247296 q_0^2 (P_0^1)^3 (P_0^2)^2 - 190080 q_0^6 (P_0^1) (P_0^2)^2 \\
& + 414720 q_0^8 (P_0^1)^3 (P_0^2) + 233472 q_0^{10} (P_0^1)^3 (P_0^2)^2 - 340992 q_0^8 (P_0^1) (P_0^2)^3
\end{aligned}$$

$$\begin{aligned}
& - 1826304 q_0^6 (P_0^1)^3 (P_0^2)^4 - 62208 q_0^4 (P_0^2)^4 + 567552 q_0^6 (P_0^1)^4 (P_0^2)^3 + 69120 q_0^4 (P_0^1)^3 (P_0^2) \\
& - 2517120 q_0^6 (P_0^2)^6 (P_0^1) + 111360 q_0^4 (P_0^2)^5 (P_0^1) - 998400 q_0^4 (P_0^1)^3 (P_0^2)^3 \\
& - 392832 q_0^6 (P_0^1)^5 + 1812480 q_0^{10} (P_0^1)^2 (P_0^2)^3 + 82944 q_0^8 (P_0^2)^4 + 743424 q_0^6 (P_0^2)^3 (P_0^1)^2 \\
& - 11836800 (P_0^1)^4 (P_0^2)^5 q_0^2 + 794880 q_0^2 (P_0^2)^5 (P_0^1)^2 + 137340 (P_0^2)^4 (P_0^1)^2 \\
& - 6856320 (P_0^1)^3 (P_0^2)^6 q_0^2 + 86400 q_0^6 (P_0^1)^3 + 6720 q_0^2 (P_0^1)^3 + 145992 (P_0^1)^3 (P_0^2)^3 \\
& - 480 q_0^2 (P_0^1) + 453120 q_0^4 (P_0^2)^6 - 1792 q_0^4 (P_0^1)^2 - 1906992 (P_0^1)^4 (P_0^2)^4 + 45360 (P_0^1)^5 (P_0^2) \\
& + 120 (P_0^2) (P_0^1) + 109824 q_0^6 (P_0^2)^5 - 5520 (P_0^1)^2 (P_0^2)^2 + 5832960 (P_0^2)^9 (P_0^1) - 4800 (P_0^2)^3 (P_0^1) \\
& + 5376 q_0^4 (P_0^2)^2 - 1714080 (P_0^2)^6 (P_0^1)^2 - 11520 q_0^6 (P_0^2)^3 + 115920 (P_0^1) (P_0^2)^5 \\
& - 610560 (P_0^1)^6 q_0^4 - 1305792 (P_0^1)^5 (P_0^2)^3 - 349056 (P_0^1)^7 (P_0^2) + 523584 q_0^2 (P_0^1)^7 \\
& - 756000 (P_0^1)^6 (P_0^2)^2 - 1365120 (P_0^1)^9 q_0^2 - \frac{2274816}{5} q_0^{10} (P_0^1)^5 + 2039040 q_0^4 (P_0^1)^8 \\
& - 622080 q_0^8 (P_0^1)^6 + 374400 q_0^6 (P_0^1)^7 + 1023840 (P_0^2) (P_0^1)^9 - 1338240 (P_0^2)^7 (P_0^1) \\
& - 2880 (P_0^1)^3 (P_0^2) + 10791720 (P_0^1)^4 (P_0^2)^6 - 395520 q_0^6 (P_0^2)^7 - 67584 q_0^{10} (P_0^2)^5 \\
& + 4617216 (P_0^1)^7 (P_0^2)^3 - 1434624 q_0^4 (P_0^2)^8 + 2490696 (P_0^1)^8 (P_0^2)^2 + \frac{49990752}{5} (P_0^2)^5 (P_0^1)^5 \\
& + 7313976 (P_0^1)^6 (P_0^2)^4 + 9979200 (P_0^1)^3 (P_0^2)^7 - 311808 q_0^8 (P_0^2)^6 + 8160000 (P_0^2)^8 (P_0^1)^2 \\
& + 73185 (P_0^2)^6 + 12726 (P_0^1)^6 + 75 (P_0^2)^2 - 3450 (P_0^2)^4 - 900 (P_0^1)^4 + 30 (P_0^1)^2 - 85320 (P_0^1)^8 \\
& - 729120 (P_0^2)^8 + 2769360 (P_0^2)^{10} + \frac{3}{5} + \frac{1096488}{5} (P_0^1)^{10} + 62208 q_0^4 (P_0^1)^4. \quad (\text{H.2})
\end{aligned}$$

I Numerical values of extrema

The positions of the extrema having the lowest free energy are shown in Table 2. Here P_0^1 , P_0^2 and q_0 are related to M_0^1 , M_0^2 and m_0 as in appendix H. Since we consider lower orders here, we can not expect clear plateaus. However at lower orders we expect that the extremum with the lowest free energy lies in the plateau and approximates the free energy well. We can check it is indeed the case for the ϕ^4 toy model.

References

- [1] J. Polchinski, “Dirichlet-branes and Ramond-Ramond charges,” Phys. Rev. Lett. **75**, 4724 (1995) [arXiv:hep-th/9510017].
- [2] J. Polchinski, “String theory,” vol.1 and 2 Cambridge monographs on mathematical physics [ISBN:0521633044].

ansatz	parameters	1st order	3rd order	5th order
SO(7)	P_0^1	0.4105507905	0.4518139994	0.4400228898
	P_0^2	0.1073836480	0.07040135462	0.06351041755
	q_0	0.4426595159	0.5126612791	0.5082289370
SO(4)	P_0^1	0.5625802884	0.6844310859	0.6695144044
	P_0^2	0.1630908715	0.08577036668	0.02122284256
	q_0	0.4713708814	0.5390149536	0.5174809839

Table 2: The positions of the extrema for each order.

- [3] J. Maldacena, “The large N limit of superconformal field theories and supergravity,” Adv. Theor. Math. Phys. **2**, 231 (1998) [Int. J. Theor. Phys. **38**, 1113 (1998)] [arXiv:hep-th/9711200].
- [4] O. Aharony, S. S. Gubser, J. Maldacena, H. Ooguri and Y. Oz, “Large N field theories, string theory and gravity,” Phys. Rept. **323**, 183 (2000) [arXiv:hep-th/9905111].
- [5] T. Banks, W. Fischler, S. H. Shenker and L. Susskind, “M theory as a matrix model: A conjecture,” Phys. Rev. D **55**, 5112 (1997) [arXiv:hep-th/9610043].
- [6] N. Ishibashi, H. Kawai, Y. Kitazawa and A. Tsuchiya, “A large- N reduced model as superstring,” Nucl. Phys. B **498**, 467 (1997) [arXiv:hep-th/9612115].
- [7] L. Smolin, “M theory as a matrix extension of Chern-Simons theory,” Nucl. Phys. B **591**, 227 (2000) [arXiv:hep-th/0002009].
- [8] T. Azuma, S. Iso, H. Kawai and Y. Ohwashi, “Supermatrix models,” Nucl. Phys. B **610**, 251 (2001) [arXiv:hep-th/0102168].
- [9] L. Smolin, “The exceptional Jordan algebra and the matrix string,” [arXiv:hep-th/0104050].
- [10] H. Aoki, S. Iso, H. Kawai, Y. Kitazawa, A. Tsuchiya and T. Tada, “IIB matrix model,” Prog. Theor. Phys. Suppl. **134** (1999) 47 [arXiv:hep-th/9908038].
- [11] J. Nishimura and F. Sugino, “Dynamical generation of four-dimensional space-time in the IIB matrix model,” [arXiv:hep-th/0111102].
- [12] D. Kabat and G. Lifschytz, “Approximations for strongly-coupled supersymmetric quantum mechanics,” Nucl. Phys. B **571**, 419 (2000) [arXiv:hep-th/9910001];

- S. Oda and F. Sugino, “Gaussian and mean field approximations for reduced Yang-Mills integrals,” JHEP **0103** 026, (2001) [arXiv:hep-th/0011175];
- F. Sugino, “Gaussian and mean field approximations for reduced 4D supersymmetric Yang-Mills integral,” JHEP **0107** 014, (2001) [arXiv:hep-th/0105284].
- [13] For example, see R. Fukuda, M. Komachiya, S. Yokojima, Y. Suzuki, K. Okumura and T. Inagaki, “Novel use of Legendre transformation in field theory and many particle systems,” Prog. Theor. Phys. Suppl. **121** (1995) 1.
- [14] E. Brezin, C. Itzykson, G. Parisi and J. B. Zuber, “Planar Diagrams,” Commun. Math. Phys. **59**, 35 (1978).
- [15] J. Nishimura and G. Vernizzi, “Spontaneous breakdown of Lorentz invariance in IIB matrix model,” JHEP **0004** 015, (2000) [arXiv: hep-th/0003223];
- “Brane world from IIB matrices,” Phys. Rev. Lett. **85**, 4664 (2000) [arXiv: hep-th/0007022];
- J. Ambjorn, K.N. Anagnostopoulos, W. Bietenholz, T. Hotta and J. Nishimura, “Monte Carlo studies of the IIB matrix model at large N,” JHEP **0007** 011, (2000) [arXiv: hep-th/0005147];
- K.N. Anagnostopoulos and J. Nishimura, “A new solution of the complex action problem and the dynamical space-time in the IIB matrix model,” [arXiv: hep-th/0108041];
- Jun Nishimura, “Exactly Solvable Matrix Models for the Dynamical Generation of Space-Time in Superstring Theory,” Phys. Rev. D **65**, 105012 (2002) [arXiv: hep-th/0108070].